CIVIL ENGINEERING STUDIES
STRUCTURAL RESEARCH SERIES NO. 168

EFFECTS OF ROADWAY UNEVENNESS ON DYNAMIC RESPONSE OF SIMPLE SPAN HIGHWAY BRIDGES

by
J. TOLEDO LEYVA
and
A. S. VELETSOS

Issued as a Part
of the
EIGHTH PROGRESS REPORT
of the
HIGHWAY BRIDGE IMPACT INVESTIGATION

UNIVERSITY OF ILLINOIS
URBANA, ILLINOIS
OCTOBER, 1958

EFFECTS OF ROADWAY UNEVENNESS ON DYNAMIC RESPONSE OF SIMPLE SPAN HIGHWAY BRIDGES

by
J. Toledo Leyva
and
A. S. Veletsos

Issued as a Part of the Eighth Progress Report of the
HIGHWAY BRIDGE IMPACT INVESTIGATION

Conducted by
THE ENGINEERING EXPERIMENT STATION
UNIVERSITY OF ILLINOIS

In Cooperation With
THE DIVISION OF HIGHWAYS
STATE OF ILLINOIS

and

U. S. DEPARTMENT OF COMMERCE
BUREAU OF PUBLIC ROADS

University of Illinois
Urbana, Illinois
October, 1958

I. INTRODUCTION

1. Object and Scope

The object of this investigation was to study analytically the influence of roadway unevenness on the dynamic response of simple span highway bridges traversed by heavy vehicles. Ordinarily, the term unevenness is used in a generalized sense to include any deviation of the bridge profile from a horizontal line passing through the supports. As used in this report, it refers to the deviations measured from the design grade. In other words, it excludes vertical curves, initial camber, or dead load deflection.

Roadway unevenness may be due to such causes as normal weathering and wear, differential settlement of the piers, shrinkage and creep of the concrete, poor construction techniques, or the presence of expansion joints. Examination of the surface conditions of actual bridges indicates that the irregularities are generally random in character. It follows then that their effects can best be described in a statistical sense, and that the most appropriate method of analyzing this problem would be through the application of random-process techniques. However, available data on the surface conditions of actual bridges are too limited to permit an analysis of this type. In this investigation the deterministic approach is used. The dynamic response of a number of bridges is evaluated for given configurations of unevenness. The following specific types are considered:

(1) A sinusoidal profile deviation, which is an example of a systematic unevenness.

(2) A profile deviation consisting of a series of half-sine waves, successively of opposite signs, having unequal wave lengths and amplitudes. Intermediate between a systematic and a random variation, this form of unevenness is referred to as semi-systematic.

(3) Two profile deviations taken from portions of actual bridge profiles.

(4) A localized irregularity in the form of a single half-sine wave.

In order to simplify the interpretation of the solutions, all analyses were made for a single axle load corresponding to the rear axle of a "typical" heavy truck the characteristics of which are given in the text. The bridges considered are of the SA-2-53 type specified by the Bureau of Public Roads[1*]; these are simple span I-beam bridges with steel girders and a concrete deck.

The results of these studies are presented in Chapters IV through VII. The method of solution and the characteristics of the bridge-vehicle systems investigated are described in Chapter III. This material is preceded by the presentation of data on the surface conditions of six actual bridges.

A brief review of available information concerning this problem[2-10] has been presented elsewhere[11].

2. Notation

The symbols used in this report are defined where they first appear in the text and are assembled here for convenient reference.

b = amplitude of a half sine wave

b/ℓ = wave parameter

ℓ = length of one half wave in a sinusoidal profile

ℓ_j = length of jth half sine wave in a semi-systematic profile ($j = 1, 2, 3$)

L = span length of beam

m = number of half-sine waves along the span of the beam

---

* Superscript numbers refer to the items in the Bibliography at the end of this report.

$\bar{m}_1$, $\bar{m}_2$ = "critical" values of m defined by Eqs. (4) and (5)

$(m_{cr})_1$, $(m_{cr})_2$ = actual "critical" values of m

T_b = natural period of vibration of the beam

T_L = natural period of vibration of the vehicle

$T_p = 2L/mv$ = "period" of the sinusoidal profile variation

v = velocity of the vehicle

x = distance from the left support to the center of a localized irregularity

$\alpha = vT_b/2L$, speed parameter

$\bar{\alpha}_1$, $\bar{\alpha}_2$ = "critical" values of α defined by Eqs. (2) and (3)

α_{cr} = actual "critical" value of α

$$\lambda = \frac{\ell_2}{\ell_2 + \ell_3}$$

$$\mu = \frac{x}{L}$$

3. Acknowledgment

The work described herein was performed as part of the Highway Bridge Impact Investigation, conducted in the Structural Research Laboratory of the Department of Civil Engineering at the University of Illinois in cooperation with the Illinois Division of Highways and the Bureau of Public Roads, U. S. Department of Commerce. This report is based on a thesis prepared by Mr. J. Toledo Leyva, under the direction of Professor A. S. Veletsos, in partial fulfillment of the requirement of the degree of Master of Science.

The authors wish to thank Professors C. P. Siess and R. K. L. Wen for helpful suggestions and comments. Special recognition is due the Highway Departments of the States of Iowa, Missouri, Nebraska and Oregon for making available for use in this study the profile data referred to in Chapter II. The cooperation accorded by these groups is gratefully acknowledged.

II. SURFACE CONDITIONS OF ACTUAL BRIDGES

4. Data for Actual Bridges

In order to provide a realistic basis for this analytical investigation, a reveiw was first made of existing data on the surface conditions of actual highway bridges. The purpose of this review was to obtain an indication of the order of magnitude of the surface irregularities present in actual bridges and of the manner in which they are likely to be distributed along the span.

The data considered were obtained from field measurements on the following six bridges:

(1) North Dillard Bridge, Oregon

(2) Troutdale Bridge, Oregon

(3) Bridge L-518 over Burris Fork, Missouri

(4) Miller's Creek Bridge, Iowa

(5) Wapsipinicon Bridge, Iowa

(6) Middle Loup River Bridge, Nebraska

Some of the profiles were determined accurately by taking elevations with a level at 10-ft. intervals, while others were obtained by means of a "roughometer machine". Representative wheel track profiles for the first five bridges are shown in Fig. 1, wherein the characteristics of the superstructures are also indicated. In this figure the diagrams for bridges (1) and (2) show the deviations of the profiles from the design or mean grade, whereas the remaining diagrams show actual profiles. For the present study the information of greatest interest is the magnitude and distribution of the differences between the actual profile and the design or mean grade line. As used in this report, the terms "unevenness" and "profile deviation" refer to these differences.

Examination of the data for the six bridges listed above shows that the distribution of the irregularities along the length of a bridge is generally random in character. However, some portions of the records examined were characterized by a reasonably systematic waviness. This somewhat vague term is used to identify a series of three or more waves, successively of opposite signs, having approximately the same length.

Throughout this report the magnitude of a systematic unevenness is measured in terms of the "wave parameter". This is defined as the ratio of the amplitude of a wave to its length. For an unevenness which is not truly systematic, the average value of the wave parameter is taken as a measure. For the profiles that were examined the average value of this parameter ranged from less than 0.001 to about 0.002.

Among the bridges considered, the North Dillard Bridge showed the largest profile deviations; these ranged approximately from -1.0 in. to 1.0 in. In general the irregularities were distributed at random. However, for a number of sections (an example is presented in Chapter VI) the unevenness was fairly systematic, and the average wave parameter was found to be about 0.002.

Although the North Dillard Bridge and the Troutdale Bridge are identical structures, the surface conditions of the two decks differed appreciably. The maximum deviations for the Troutdale Bridge were about 0.5 in., but occurred gradually over a great length.

The deck surface of Bridge L-518 over Burris Fork was fairly smooth. The maximum deviations from the mean were of the order of $\pm$ 0.2 in. The sections of the span that presented a more or less systematic waviness had an average wave parameter of about 0.0015.

The profile of the Miller's Creek Bridge was characterized by a well defined waviness that was distributed along the entire span. The

deviations ranged from -0.2 in. to + 0.2 in., and the average wave parameter was of the order of 0.0015.

The surfaces of the Wapsipinicon River Bridge and the Middle Loup River Bridge were smooth.

III. SYSTEMS ANALYZED AND METHOD OF ANALYSIS

5. Types of Bridges and Vehicles Considered

The bridges considered in this study correspond to the SA-2-53 type specified in the "Standard Plans for Highway Bridge Superstructures" of the Bureau of Public Roads[1]. These are I-beam bridges with steel girders and a concrete deck, designed for H20-S16 loading. In this report these structures are referred to as "typical" I-beam bridges. Their weights and natural frequencies, calculated from data given in the aforementioned manual, are listed in Table 1. A detailed description of the characteristics of the surface unevenness considered in the various phases of this investigation is given in subsequent sections.

In order to simplify the interpretation of the results, the vehicle was represented by a single axle load. It should be noted, however, that in general, the response obtained with such a load is not appreciably different from that due to a typical two-axle truck loading. Unless specified differently, the single axle load considered is the rear axle of a "typical" truck, the characteristics of which are listed in Table 2.

6. Method of Analysis

All numerical results were obtained on the ILLIAC, the electronic digital computer of the University of Illinois, using the program developed by R. K. L. Wen[10].

In the analysis of the system the bridge is represented as a simply supported elastic beam of uniform mass and cross section. In turn, the beam is treated as a system having a single degree of freedom. Specifically, it is assumed that the deflected configuration of the beam at any time is proportional to the static configuration produced by the weight of the vehicle and

TABLE 1 CHARACTERISTICS OF "TYPICAL" BRIDGES

Span (ft.)	Total Weight (lb.)	Fundamental Nat. Frequency* (c.p.s.)	$\frac{T_b}{2L}$ (sec./ft.)
20	98,000	12.13	0.00206
45	227,000	5.41	0.00206
60	323,500	4.08	0.00204
70	385,700	3.19	0.00224
78	448,200	2.81	0.00228
90**	481,000	2.58	0.00216

* Complete composite action is assumed between the concrete slab and the I-beams.

** Since the largest simple span specified in the Standard Plans of the Bureau of Public Roads is 78 ft. long, the characteristics of this span were determined by extrapolation.

TABLE 2 CHARACTERISTICS OF "TYPICAL" TRUCK

	Rear Axle		Front Axle
Sprung Weight (lb.)	26,000		7,700
Unsprung Weight (lb.)	5,100		1,200
Spring Constant (lb./in.)	21,700		2,700
Frequency (c.p.s.)	2.86		1.85
Axle Spacing (ft.)		14	
Gross Vehicle Weight (lb.)		40,000	

the weight of the beam itself. It is further assumed that the vehicle moves at a constant speed and that, while on the span, at no time does it lose contact with the bridge. Also, damping for the vehicle and the bridge is neglected.

For the present study, the vehicle is assumed to have no vertical motion as it enters the span, and the bridge is considered to be initially at rest but deflected under its own weight. In all the problems the unevenness was measured with reference to this initially deflected configuration. In other words, the design grade was assumed to coincide with the dead load deflection configuration of the structure.

IV. EFFECTS OF A SINUSOIDAL UNEVENNESS

7. General

This part of the investigation included the solution of the three series of problems outlined in the following paragraphs. In all cases, the first half-sine wave was assumed to be located below the mean grade line.

First Series This series comprised solutions for spans of 20, 45, 60, 70, 78 and 90 ft. The variables considered were the speed of the vehicle and the number of waves present along the span. The vehicle speed was varied approximately from 15 mph to 70 mph at increments of 2.5 mph. For the majority of cases the number of half-waves considered is 0 (smooth surface), 3, 5, 7, 9 and 15, but in several instances solutions were also obtained for additional numbers of waves. For this series of problems the wave parameter, b/ℓ, was equal to 0.001.

Second Series The solutions obtained in this case were for spans of 20 and 45 ft and a wave parameter of 0.003. As before, the speed of the vehicle was varied from 15 to 70 mph at increments of 2.5 mph.

Third Series For this series of problems the speed parameter α, defined by Eq. 1 in the next section, was taken equal to 0.10. Solutions were obtained for spans of 20, 45, 60, 70, 78 and 90 ft. The number of half-waves along each span was varied from 0 to 15 at increments of one, with the wave parameter taken as 0.001.

8. First Series of Problems

8.1 Presentation of Results The results obtained from this series of problems are given in Figs. 2 through 7. In Fig. 2 the amplification factors for maximum bending moment at midspan of the 20-ft span are plotted as a function of the speed parameter α. The amplification factor designates

the ratio of the dynamic effect at a point to the corresponding maximum static effect. The speed parameter is defined by the equation

$$\alpha = \frac{vT_b}{2L} \qquad (1)$$

in which v denotes the velocity of the vehicle, L the span length and T_b the fundamental natural period of vibration of the unloaded bridge. The number associated with each curve identifies the number of half-waves present along the length of the bridge. Similar plots for spans of 45, 60, 70, 78 and 90 ft are given in Figs. 3 through 7, respectively.

For the 20-ft span, it can be seen that the influence of the unevenness is quite small. The difference between the peak amplification factors for an uneven surface and a smooth surface is of the order of 0.10. It is further noticed that the curves corresponding to different numbers of waves have similar shape and are in phase with one another.

For the spans of 60, 70, 78 and 90 ft, one finds no resemblance between the curves corresponding to an uneven surface and a smooth surface. The peaks of the various curves are generally out of phase, with the value of α corresponding to a peak decreasing as the number of waves increases. The dynamic increments due to surface unevenness are appreciable in this case, and they tend to increase with increasing span length. For example, for the 60-ft span the difference between the peak amplification factors for the most severe unevenness considered and the smooth surface is about 0.45. The corresponding difference for the 70-ft span is 0.50, while for the 78-ft and 90-ft spans it is about 0.80.

The results for the 45-ft span represent a condition intermediate between the two conditions described above.

8.2 Critical Speed Parameters As pointed out elsewhere[10], one might expect two conditions under which the dynamic effects due to a sinusoidal profile deviation may be of appreciable magnitude. The first corresponds to the case in which the "period" of the profile, T_p, (i.e., the time required for the load to travel over the distance covered by one complete wave) coincides with the natural period of vibration of the load, T_L. The value of α corresponding to this "critical" condition is denoted by $\bar{\alpha}_1$ and given by the expression

$$\bar{\alpha}_1 = \frac{1}{m} \frac{T_b}{T_L} \quad , \tag{2}$$

where m is the number of half-waves present along the span, and T_b and T_L are as previously defined.

The second "critical" condition may be expected when the period of the profile coincides with the fundamental natural period of the bridge. Designated as $\bar{\alpha}_2$, the value of α corresponding to this condition is given by the expression

$$\bar{\alpha}_2 = \frac{1}{m} \quad . \tag{3}$$

When $T_b = T_L$, $\bar{\alpha}_1 = \bar{\alpha}_2$.

The values of α corresponding to the peaks of the curves in Figs. 3 through 7 are listed in Table 3; these are designated as α_{cr}. Included in this table for purposes of comparison are also the values of $\bar{\alpha}_1$ and $\bar{\alpha}_2$ evaluated from Eqs. (2) and (3). It is to be emphasized that α_{cr} corresponds to the absolute peak value of a curve within the range of velocities considered. This peak does not necessarily occur at the value of α for which there is the maximum difference between the curves for an uneven surface and a smooth surface.

TABLE 3 COMPARISON OF VALUES OF α_{cr}, $\bar{\alpha}_1$ AND $\bar{\alpha}_2$

WAVE PARAMETER $b/\ell = 0.001$

No. of Half Waves	L = 45' $\frac{T_b}{T_L} = 0.529$			L = 60' $\frac{T_b}{T_L} = 0.701$			L = 70' $\frac{T_b}{T_L} = 0.897$			L = 78' $\frac{T_b}{T_L} = 1.018$			L = 90' $\frac{T_b}{T_L} = 1.108$		
	α_{cr}	$\bar{\alpha}_1$	$\bar{\alpha}_2$	α_{cr}	$\bar{\alpha}_1$	$\bar{\alpha}_2$	α_{cr}	$\bar{\alpha}_1$	$\bar{\alpha}_2$	α_{cr}	$\bar{\alpha}_1$	$\bar{\alpha}_2$	α_{cr}	$\bar{\alpha}_1$	$\bar{\alpha}_2$
3	0.188	0.176	0.333*	0.217	0.234*	0.333*	0.229	0.299*	0.333*	0.234	0.339*	0.333*	0.229	0.369*	0.333*
5	0.076	0.106	0.200	0.124	0.140	0.200	0.154	0.179	0.200	0.180	0.204	0.200	0.178	0.222	0.200
7	0.090	0.076	0.143	0.106	0.100	0.143	0.129	0.128	0.143	0.149	0.146	0.143	0.136	0.158	0.143
9	0.058	0.059	0.111	0.073	0.078	0.111	0.093	0.100	0.111	0.112	0.113	0.111	0.109	0.123	0.111
15	0.159	0.035*	0.067	0.046	0.047	0.067	0.057	0.060	0.067	0.062	0.068	0.067	0.071	0.074	0.067

*These values do not fall within the range of α's considered; therefore, the values of α_{cr} and $\bar{\alpha}_1$ (or $\bar{\alpha}_2$) cannot be compared.

Referring to the results given in Table 3 for 45, 60 and 70-ft spans, it can be seen that while there is a reasonable degree of agreement between the values of α_{cr} and $\bar{\alpha}_1$, there appears to be no correspondence between the values of α_{cr} and $\bar{\alpha}_2$. It follows that the condition of synchronization between the period of the profile deviation and the natural period of vibration of the load is the more severe of the two "critical" conditions mentioned before. For the 78-ft and 90-ft spans, the values of $\bar{\alpha}_1$ and $\bar{\alpha}_2$ are of the same order of magnitude and, therefore, it is not possible to assess the relative importance of the two conditions. The results for the 20-ft span are not included in this comparison because the magnitude of the effects are quite small in this case.

8.3 Magnitude of Dynamic Effect The dynamic increments for the various cases considered can be determined from the curves given in Figs. 2 through 7. As already noted, the magnitude of these increments increases as the span length increases. This trend may be attributed to the following two factors: (a) Since the wave parameter is constant for all span lengths, the amplitude of the wave corresponding to a fixed value of m is greater for the longer spans. (b) As the span length increases, the ratio T_b/T_L approaches unity with the result that at a "critical" speed the period of the surface unevenness is in synchronism with both the natural period of the vehicle and the natural period of the bridge. That this is a most precarious condition is physically apparent.

9. Second Series of Problems

These problems were considered in order to investigate the effect of increasing the amplitude of the surface deviation for bridges of short spans. The solutions obtained were for spans of 20 and 45 ft and a wave parameter of 0.003.

The results are presented in Figs. 8 and 9. It can be seen that, in this case, the dynamic increments are appreciable. For the 20-ft span the maximum difference between the peak values of the curves for the uneven surface and the smooth surface is about 0.35. For the 45-ft span the corresponding difference is 0.70.

In Table 4 the values of α_{cr} are compared with the values of $\bar{\alpha}_1$ and $\bar{\alpha}_2$ determined from Eqs. (2) and (3). For the 45-ft span $\alpha_{cr} \simeq \bar{\alpha}_1$ and the results confirm those presented in the preceding sections. For the 20-ft span $\alpha_{cr} \simeq \bar{\alpha}_2$, indicating that, in this case, the maximum response is obtained when the period of the profile deviation is close to the natural period of vibration of the bridge. However, it should be noted that the values of $\bar{\alpha}_1$ are less than the minimum values of α for which solutions were obtained.

TABLE 4 COMPARISON OF VALUES OF α_{cr}, $\bar{\alpha}_1$ AND $\bar{\alpha}_2$

WAVE PARAMETER $b/\ell = 0.003$

No. of Half Waves	L = 20' $\frac{T_b}{T_L} = 0.236$			L = 45' $\frac{T_b}{T_L} = 0.529$		
	α_{cr}	$\bar{\alpha}_1$	$\bar{\alpha}_2$	α_{cr}	$\bar{\alpha}_1$	$\bar{\alpha}_2$
5	0.190	0.047	0.200	0.106	0.106	0.200
7	0.141	0.034	0.143	0.091	0.076	0.143
9	0.113	0.026	0.111	0.060	0.059	0.111

10. Third Series of Problems

In order to further substantiate the observations made in the preceding sections, additional solutions were obtained for the particular value of $\alpha = 0.10$. These solutions are summarized in Fig. 10. In this figure the

amplification factors for maximum bending moment at midspan of six different bridges are plotted as a function of the number of half-sine waves present along the span. The wave parameter b/ℓ is taken equal to 0.001.

The values of m corresponding to the two conditions of synchronization referred to previously are denoted by $\bar{m}_1$ and $\bar{m}_2$, and are given by the equations

$$\bar{m}_1 = \frac{1}{\alpha}\frac{T_b}{T_L} \qquad (\text{when } T_p = T_L) \tag{4}$$

$$\bar{m}_2 = \frac{1}{\alpha} \qquad (\text{when } T_p = T_b). \tag{5}$$

When $T_b = T_L$, $\bar{m}_1 = \bar{m}_2$.

For the problems considered, the values of $\bar{m}_1$ and $\bar{m}_2$ are listed in part (a) of Table 5. Included also for comparison are the values of m corresponding to the two peaks of the curves given in Fig. 10. These values are designated as $(m_{cr})_1$ and $(m_{cr})_2$. For the three longest spans there is only one peak, so that $(m_{cr})_1 = (m_{cr})_2$. It can be seen that the agreement between predicted and actual critical values is quite satisfactory.

Returning now to Fig. 10 it should be noticed that, with the exception of the 20-ft span, the magnitude of the response for $\bar{m}_1$ is larger than that for $\bar{m}_2$. It should also be noticed that the peak response increases as the span length increases or, more precisely, as the natural periods of vibration of the vehicle and the bridge become equal.

In Fig. 11 are summarized the results of a similar study for a vehicle having a natural period of vibration of 0.28 sec. For the results presented thus far the natural period of the vehicle was 0.35 sec. It is noteworthy that in this case the curve for the 78-ft span has two peaks, whereas the corresponding curve given in Fig. 10 has a single peak. This difference

arises from the fact that when $T_L = 0.28$ sec. the values of $\bar{m}_1$ and $\bar{m}_2$ are not as close together as when $T_L = 0.35$ sec. The predicted and actual values of m_{cr} are compared in part (b) of Table 5. As in previous cases, the comparison is satisfactory.

TABLE 5 COMPARISON OF m_{cr} VALUES, $\alpha = 0.10$

Span ft	$\frac{T_b}{T_L}$	$(m_{cr})_1$	$\bar{m}_1$	$(m_{cr})_2$	$\bar{m}_2$
	(a) For $T_L = 0.35$ sec.				
20	0.236	1.8	2.4	9.8	10.0
45	0.529	6.0	5.3	10.5	10.0
60	0.701	6.0	7.0	11.0	10.0
70	0.897	8.8	9.0	8.8	10.0
78	1.018	10.0	10.2	10.0	10.0
90	1.108	10.0	11.1	10.0	10.0
	(b) For $T_L = 0.28$ sec.				
20	0.294	2.0	2.9	10.0	10.0
45	0.660	6.0	6.6	10.7	10.0
60	0.875	8.8	8.7	8.8	10.0
70	1.120	10.4	11.2	10.4	10.0
78	1.270	13.0	12.7	11.0	10.0

The second noteworthy feature of the curves given in Fig. 11 is that the peak value of the amplification factor for the 78-ft span is smaller than that for either the 60-ft or 70-ft span. This result confirms the assertion made previously to the effect that the maximum response is obtained when the ratio of the natural periods of the vehicle and the bridge are close to unity.

11. Absolute Maximum Effects at Midspan

11.1 Presentation of Results The curves presented in Figs. 2 through 9 illustrate the influence of the speed of the vehicle on the maximum response of the bridge. The detailed characteristics of these curves, although interesting, are of little practical value. Inasmuch as in an actual application the speed of the vehicle may have any value within the range considered, the most significant information is provided by the peak values of these curves.

For the first series of problems, the peak amplification factors for maximum bending moment at midspan are plotted in Fig. 12a as a function of the number of half-sine waves present along the span. The range of speeds considered is from 15 mph to 70 mph; the wave parameter is 0.001. Similar curves for the peak amplification factors for maximum deflection at midspan are given in Fig. 12b. These were obtained from plots similar to those given in Figs. 2 through 7. The curves given in Figs. 13a and 13b correspond to a range of velocities from 15 to 45 mph, instead of from 15 to 70 mph.

11.2 Discussion The most striking characteristic of the results presented in Figs. 12 and 13 is the order of magnitude of the amplification factors. Although the magnitude of the surface irregularities considered in these solutions is by no means excessive, the dynamic effects are fairly large. In interpreting the significance of these results it is important to remember that damping in the vehicle and the bridge was neglected in arriving at these solutions. Accordingly, the computed effects are generally greater than those to be expected in a practical application. The influence of damping is likely to be most important when the number of waves along the span is large and when the natural periods of vibration of the vehicle and the bridge are close to one another.

For the results given in Figs. 12 and 13, b/ℓ is the same for all span lengths and all values of m. Consequently, as m increases, ℓ decreases and b increases. It follows further that, with m fixed, b increases with increasing span length. A more direct comparison is presented in Fig. 14.

For the three spans considered in this figure the values of b/ℓ have been selected so that, for constant m, the amplitudes of the waves are identical. In particular, b/ℓ is equal to 0.001, 0.0016 and 0.0035 for the spans of 70, 45 and 20 ft, respectively. This corresponds to the satisfaction of the following relationship for all three cases:

$$mb = 0.84$$

where b is expressed in inches. It is important to notice that, even when the response of the three spans is compared on the basis of fixed values of mb, the maximum response is obtained for the longest span for which the natural period of vibration is closest to that of the vehicle.

It is noted in passing that in Fig. 14 the curves for the spans of 20 and 45 ft were determined by interpolation. As explained in Section 9, in addition to the solutions corresponding to $b/\ell = 0.001$, solutions were available for $b/\ell = 0.003$ for a number of different values of m. From these data the linear relationships given in Fig. 15 were established. These lines were used to effect the necessary interpolations and extrapolation. When there was no solution available for $b/\ell = 0.003$, a linear relationship was assumed with a slope equal to the average slope of the lines in Fig. 15.

V. EFFECTS OF A SEMI-SYSTEMATIC UNEVENNESS

12. General

The surface unevenness considered in this section consists of five consecutive half-sine waves, alternately of opposite signs, having different lengths and amplitudes. The length of each end wave is taken equal to one-fifth the length of the span, whereas the lengths of the remaining waves are varied over the entire possible range, always keeping the waves symmetrical about the center line of the span. For each wave, the amplitude-to-length ratio (i.e., the wave parameter) is considered to be constant.

The distribution of the unevenness can conveniently be specified in terms of the dimensionless parameter λ, defined as

$$\lambda = \frac{\ell_2}{\ell_2 + \ell_3} \tag{6}$$

where ℓ_2 and ℓ_3 are the lengths of the second and the third waves, respectively. The range of λ is from 0 to 1. As shown in Fig. 16, $\lambda = 0$ corresponds to the case in which there are only three waves along the span, while $\lambda = 1.0$ corresponds to the case in which there are four waves. For a sinusoidal unevenness $\lambda = 0.5$. The end waves are assumed to be located below the grade line.

Solutions were obtained for spans of 20, 45 and 70 ft for values of λ from 0 to 1.0 and a range of speeds from 15 mph to 70 mph. The wave parameter was taken as 0.001 for the 70-ft span and as 0.003 for the 45-ft and 20-ft spans.

13. Presentation and Discussion of Results

The results of this part of the investigation are presented in Figs. 17 through 20b. In Figs. 17 through 19 the amplification factors for maximum bending moment at the center of the three spans are given as a function of α for various values of the profile parameter λ. The peak values of these curves are

plotted in Fig. 20a as a function of λ. Similar plots for absolute maximum deflection are given in Fig. 20b. For purposes of comparison the results for a smooth surface are also indicated in these figures.

It is important to notice that for a fairly wide range of values of λ the ordinates of the curves in Figs. 20 are of the same order of magnitude as the corresponding ordinates for a sinusoidal profile ($\lambda = 0.50$). This is particularly true in the case of the 70-ft span for which the natural periods of the bridge and the vehicle are close to one another. For this span, the amplification factor for bending moment varies from 1.85 to 1.97 for values of λ in the range between 0.15 and 1.0. The corresponding range of variation of the amplification factor for deflection is from 2.2 to 2.4.

The practical implication of these results is that, even when the unevenness of a bridge deck is not entirely systematic, it may be possible to estimate its effects by considering a sinusoidal unevenness having approximately the same number of waves and an amplitude corresponding to the average wave parameter of the actual profile.

VI. EFFECTS OF ACTUAL BRIDGE PROFILES

14. General

The surface irregularities used in the solutions presented in this section were determined from field measurements on actual bridges. The solutions given are for a "typical" 70-ft span traversed by a "typical" vehicle at speeds ranging from 15 mph to 70 mph. Two distributions of deck unevenness are considered.

The first corresponds to a section of the profile of the North Dillard Bridge. The particular profile used was taken along a line 8.5 ft east of, and parallel to, the center line of the roadway, beginning at the South Interior Pier and extending 70 ft to the north. The surface unevenness was then considered to be equal to the deviations of this profile from a straight line passing through the end points of the 70-ft segment. A sketch of the unevenness together with a tabulation of the ordinates at intervals of 8.4 in. is given in Fig. 21. The ordinates of points below the reference line are taken as positive. It should be noticed that there are four distinct half-waves present along this 70-ft segment. The value of the average wave parameter is about 0.002.

The second distribution corresponds to a section of the Miller's Creek Bridge. As previously noted, this is a three-span continuous structure with a central span of 70 ft. The profile used was taken on the central span along a line 3 ft east of the center line of the roadway. As in the preceding case, the unevenness was measured with reference to a straight line passing through the end points of the 70-ft segment. The results are tabulated in Fig. 22. There is a distinct waviness in this diagram. The exact number of half-waves present is difficult to identify, but it appears to be between 10 and 12. The value of the average wave parameter is approximately 0.0015.

15. Presentation and Discussion of Results

In Fig. 23 the amplification factors for maximum bending moment at the center of the 70-ft span are plotted as a function of the speed parameter for each of the two profiles considered. The curves (a) and (b) are similar to those in Fig.5b for a sinusoidal unevenness with m = 4 and m = 10 or 12, respectively.

TABLE 6 COMPARISON OF RESPONSE FOR ACTUAL AND SINUSOIDAL PROFILES

Bridge Profile	α_{cr}	Max. A.F.
North Dillard Bridge	0.213	2.30
Sinusoidal; m = 4; b/ℓ = 0.001	0.182	1.84
Miller's Creek Bridge	0.066	2.08
Sinusoidal; m = 10; b/ℓ = 0.001	0.082	1.91
Sinusoidal; m = 12; b/ℓ = 0.001	0.072	1.70

In Table 6 the critical values of α for the actual profiles are compared with the values corresponding to the sinusoidal profiles indicated in the table. The agreement between the two sets of results is satisfactory. Included also are the amplification factors for absolute maximum moment at midspan. It can be seen that, in this case, the values for the actual profiles are greater than for the sinusoidal profiles. This difference can be explained by the fact that the wave parameter of the sinusoidal profiles is 0.001, whereas, as previously noted, the average wave parameters for the North Dillard Bridge and the Miller's Creek Bridge are 0.002 and 0.0015.

The results obtained for a sinusoidal profile by extrapolating linearly to the appropriate values of the wave parameter are found to be in good agreement with those obtained for the actual profiles. These results confirm the

assertion made in Article 13 concerning the influence of a semi-systematic unevenness. The indications are that the concept of the equivalent sinusoidal unevenness may be used to arrive at an order-of-magnitude estimate of the dynamic increments due to a wavy bridge surface.

VII. EFFECTS OF A LOCALIZED UNEVENNESS

16. General

In this section are presented the results of an exploratory study on the effects of a localized irregularity having the form of a half-sine wave. The wave is assumed to project above the grade line, and its length is taken equal to one-fifth the length of the span. The solutions are for a 70-ft. span; the irregularity is assumed to occupy successively the first, the second and the third fifth of the span.

17. Presentation of Results

The results of this study are given in Figs. 24 through 27. In Figs. 24 through 26 are plotted the amplification factors for maximum bending moment at midspan as a function of α. Identified as positions (1), (2) and (3), the three positions of the wave are shown at the upper left corner of the figures. Fig. 24 corresponds to a wave parameter of 0.001, while Figs. 25 and 26 correspond to wave parameters of 0.002 and 0.003, respectively. In each figure, the curve corresponding to a smooth surface is also included for purposes of comparison.

The maximum values of the curves given in Figs. 24 through 26 are summarized in Fig. 27. The abscissa μ in this figure denotes the ratio of the distance between the left support and the center of the irregularity divided by the span length.

It can be seen that when $b/\ell = 0.001$ the maximum response does not differ greatly from that corresponding to a smooth surface. For $b/\ell = 0.002$ the peak response occurs for $\mu = 0.30$, and it is equal to that obtained for a continuous sinusoidal unevenness having the same length but an amplitude one-half as great. In all cases the response decreases sharply as μ approaches

the value of 0.50. This decrease can be explained as follows. The primary effect of the irregularity is to amplify the vertical oscillation of the vehicle. However, if the irregularity is situated close to midspan, by the time the oscillation of the vehicle is magnified the vehicle has crossed the center of the span and is in a region where it cannot produce large effects.

This study has been of an exploratory nature. Needless to say, additional studies are required to assess the contribution of the various factors entering into this problem.

VIII. CONCLUSION

18. Summary of Results

The purpose of this investigation was to obtain numerical solutions depicting the influence of roadway unevenness on the dynamic response of a number of simple span highway bridges. Four different distributions of surface irregularities were considered.

The parameters used to describe the influence of a sinusoidal unevenness include the number of waves present along the span, the wave parameter b/ℓ, the speed parameter α, and the ratio of the natural periods of vibration of the bridge and the vehicle, T_b/T_L. With a few exceptions, the results obtained correspond to a value of $b/\ell = 0.001$.

When T_b/T_L is greater than about 0.25, the maximum response is attained at the speed for which the "period" of the profile variation, T_p, is approximately equal to the natural period of vibration of the vehicle. When T_b/T_L is of the order of 0.25 or less the maximum response may occur when $T_p \simeq T_b$. Other things being equal, the magnitude of the maximum response increases as the ratio T_b/T_L approaches unity. For the problems analyzed, the amplification factors for absolute maximum moment and deflection at midspan are summarized in Figs. 12a through 14. For b/ℓ greater than 0.001, there appears to be a linear relationship between the wave parameter and the maximum response of the bridge.

A number of solutions were obtained for a semi-systematic unevenness consisting of five consecutive half-sine waves of different amplitudes and lengths, and also for two profiles determined from field measurements on actual bridges. These solutions show that the magnitude of the peak response is not very sensitive to the details of the unevenness and suggest that, when judiciously interpreted, the results for the sinusoidal unevenness may be used to

arrive at an order-of-magnitude estimate of the dynamic increments produced by a wavy bridge surface.

Although the magnitude of the irregularities considered in the present investigation was small, the magnitude of the computed effects was quite large. While it can reasonably be concluded that unevenness of the bridge deck may indeed be a source of large dynamic effects, it is important to note that the influence of damping was neglected in arriving at the present results. Damping is likely to play an important role in the case of a reasonably systematic unevenness, particularly when the number of waves present along the span is large and the period of the unevenness and the natural periods of vibration of the bridge and the vehicle are close to each other. The extent of this influence has not been investigated as yet.

BIBLIOGRAPHY

1. "Standard Plans for Highway Bridge Superstructures" Bureau of Public Roads, Washington, D. C., 1953.

2. "Preliminary Impact Studies -- Skunk River Bridge on the Lincoln Highway near Ames, Iowa", by A. H. Fuller, Bulletin No. 63, Iowa State College, Engineering Experiment Station, 1922.

3. "Tests on Rolled-Beam Bridge Using H20-S16 Loading", by G. M. Foster, Research Report 14-B, Highway Research Board, National Research Council, Publication No. 253, 1952, p. 10.

4. "Second Progress Report, Highway Bridge Impact Investigation", Civil Engineering Studies, Structural Research Series No. 24, University of Illinois, 1952.

5. "Dynamic Load Analysis and Design of Highway Bridges", by C. F. Scheffey, Bulletin 124, Highway Research Board, National Research Council, Publication No. 411, 1956, p. 16.

6. "Vibration and Deflection of Rolled-Beam and Plate-Girder Bridges", by G. M. Foster and L. T. Oehler, Bulletin 124, Highway Research Board, National Research Council, Publication No. 411, 1956, p. 79.

7. "Vibration Measurements on Simple Span Bridges", by J. M. Biggs and H. S. Suer, Bulletin 124, Highway Research Board, National Research Council, Publication No. 411, 1956, p. 1.

8. "Vibration Study of Three-Span Continuous I-Beam Bridge", by J. M. Hayes and J. A. Sbarounis, Bulletin 124, Highway Research Board, National Research Council, Publication No. 411, 1956, p. 47.

9. "Dynamic Stresses in Continuous Plate-Girder Bridges", by R. C. Edgerton and G. W. Beecroft, Paper 973, Journal of the Structural Division of the ASCE, Vol. 82, No. ST 3, May 1956, p. 973-1.

10. "Dynamic Behavior of Simple Span Highway Bridges Traversed by Two-Axle Vehicles", by R. K. L. Wen, Structural Research Series Report No. 142, University of Illinois, 1957.

11. "Seventh Progress Report -- Highway Bridge Impact Investigation" Part B by J. Toledo, University of Illinois, 1957.

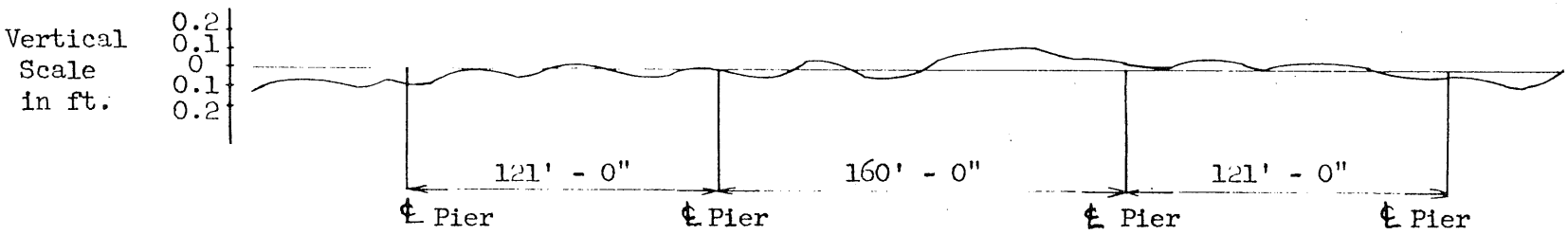

1a NORTH DILLARD BRIDGE (402 ft. Three Span Continuous Plate Girder)
Deviations from True Grade
Profile Taken at a Section 8'-6" East of ℄ of Roadway

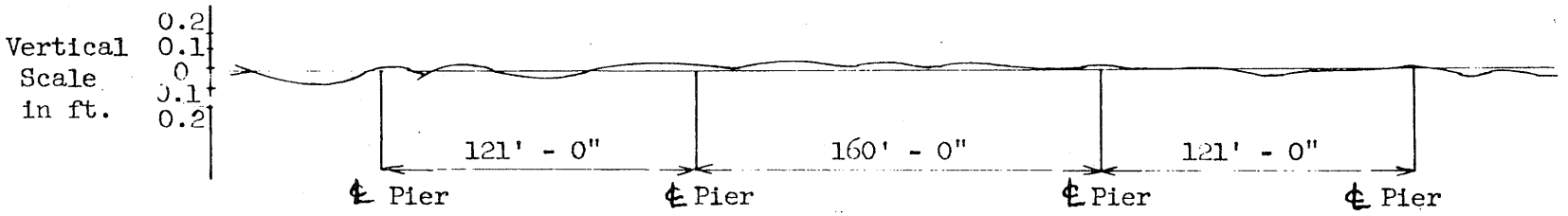

1b TROUTDALE BRIDGE (402 ft. Three Span Continuous Plate Girder)
Deviations from True Grade
Profile Taken at a Section 3'-6" North of the ℄ of Roadway

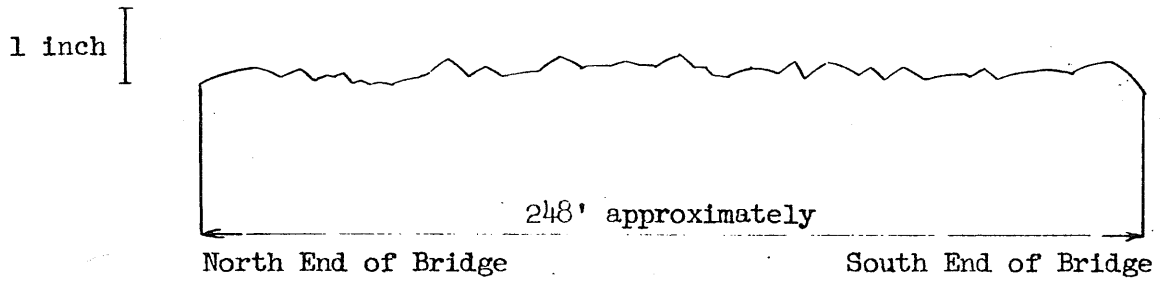

1c BRIDGE L-518 OVER BURRIS FORK
Profile Taken at a Section 2' East of ℄ of Roadway

FIG. 1 TYPICAL PROFILES OF ACTUAL BRIDGES

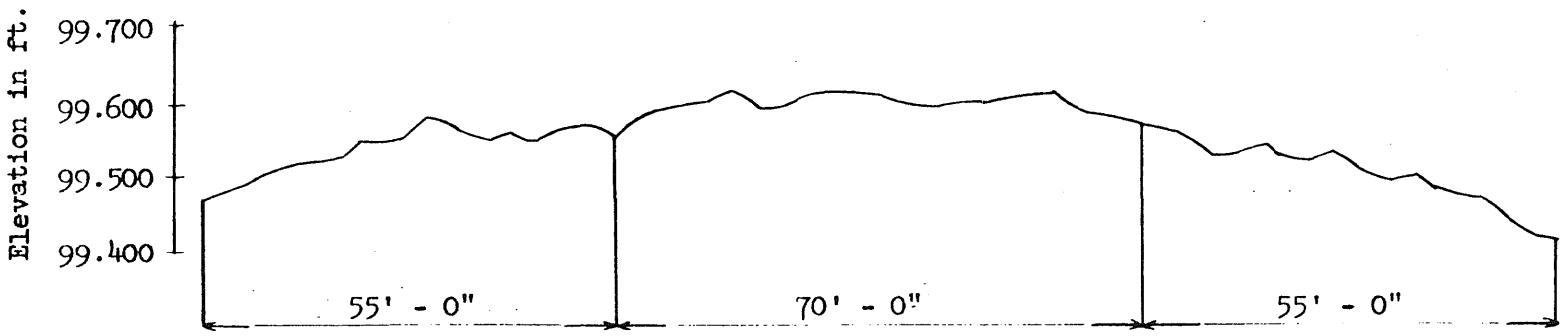

1d MILLER'S CREEK BRIDGE (180 ft. Three Span Continuous I-Beam)
Profile Taken at a Section 3' East of ℄ of Roadway

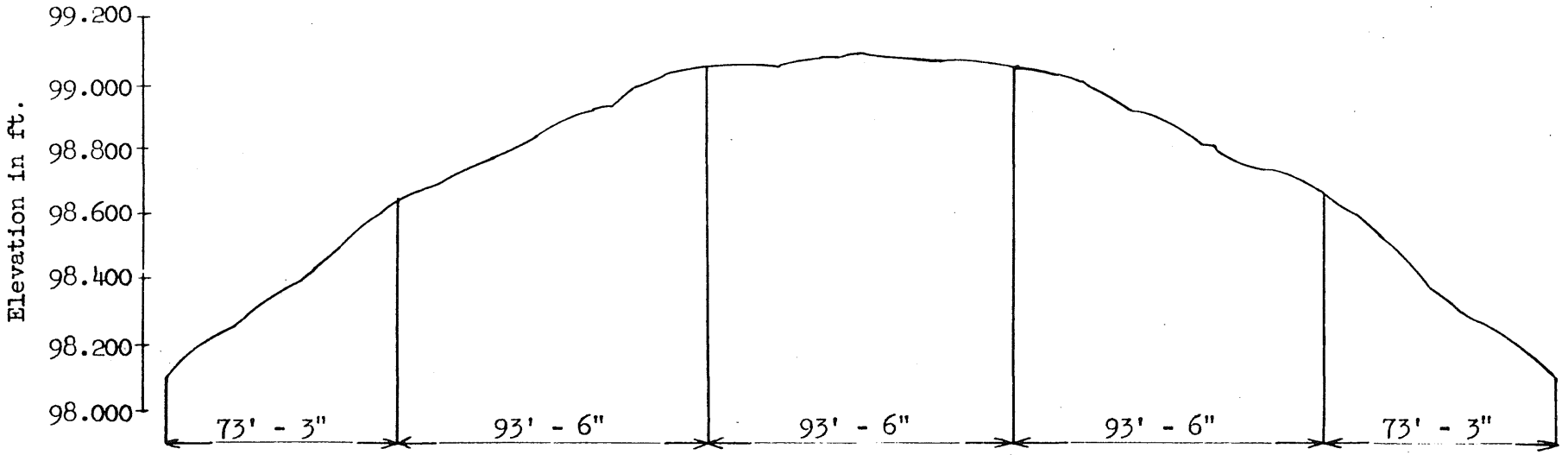

1e WAPSIPINICON RIVER BRIDGE (427 ft. Five Span Continuous I-Beam)
Profile Taken at a Section 3' North of ℄ of Roadway

FIG. 1 (Cont.) TYPICAL PROFILES OF ACTUAL BRIDGES

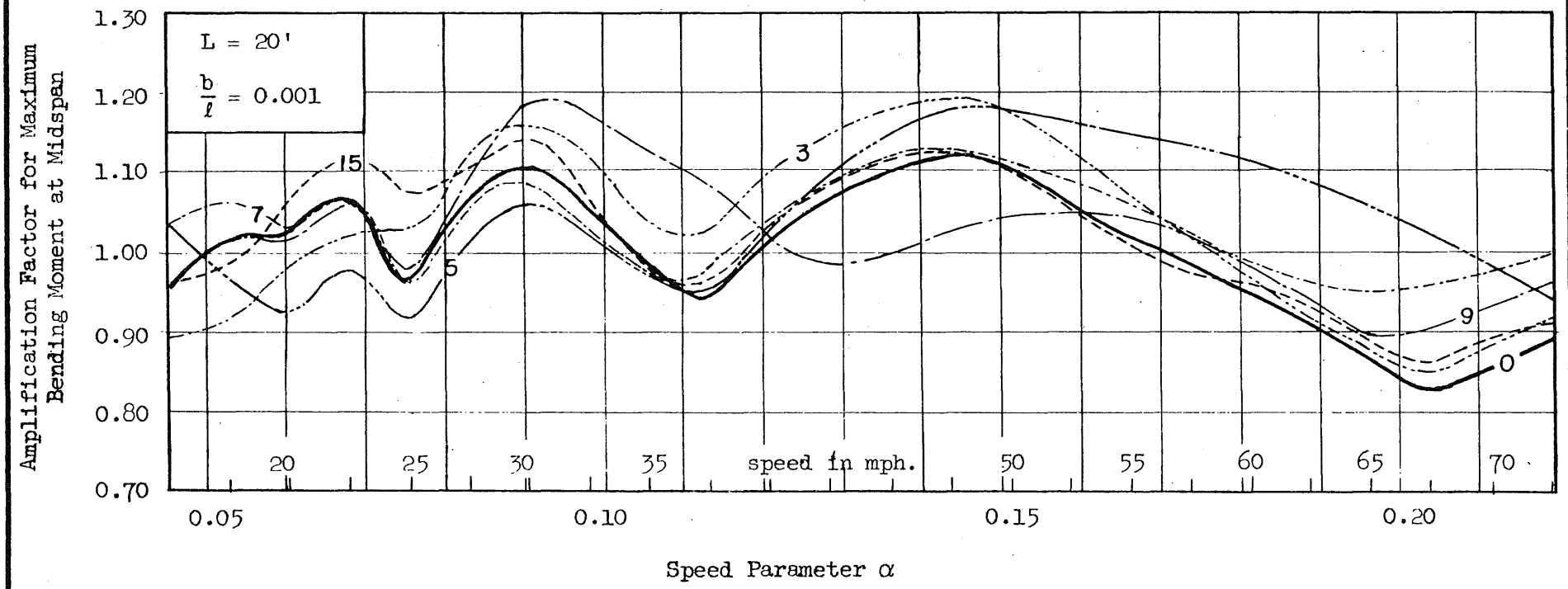

FIG. 2 EFFECT OF VELOCITY, SINUSOIDAL PROFILE

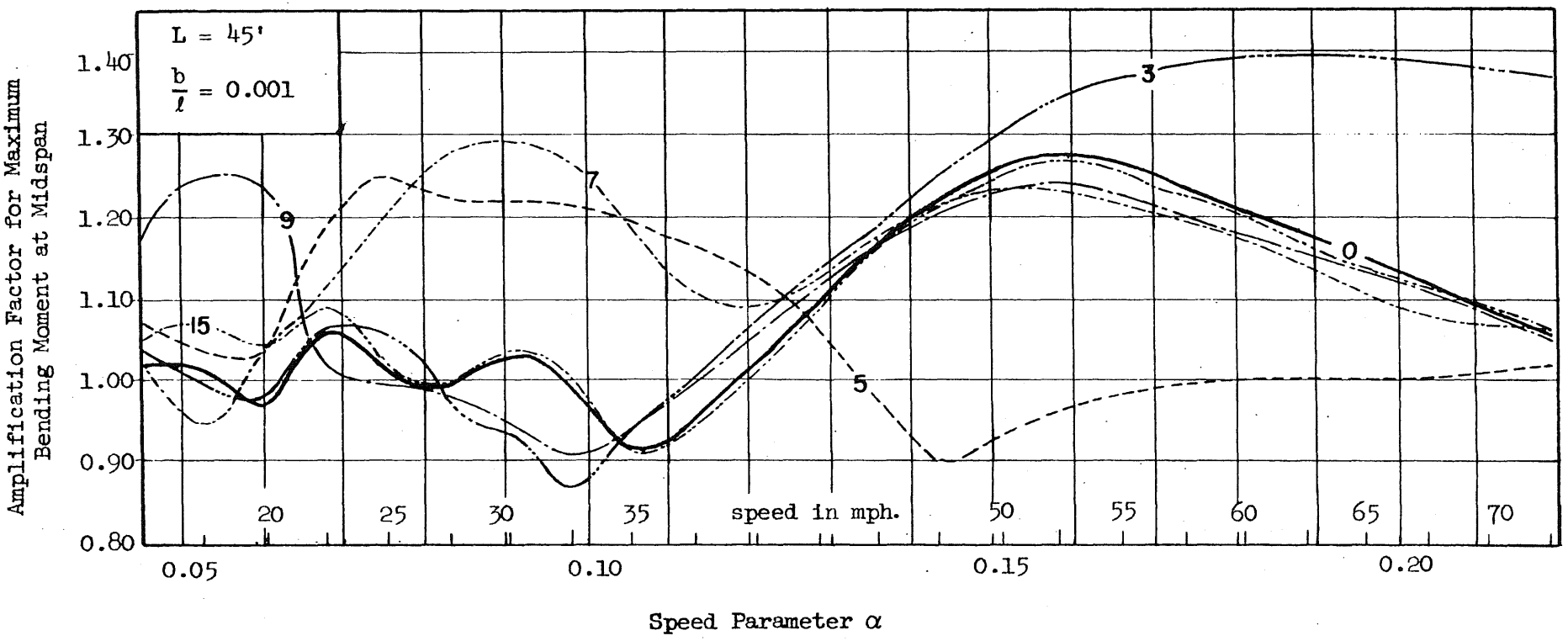

FIG. 3 EFFECT OF VELOCITY, SINUSOIDAL PROFILE

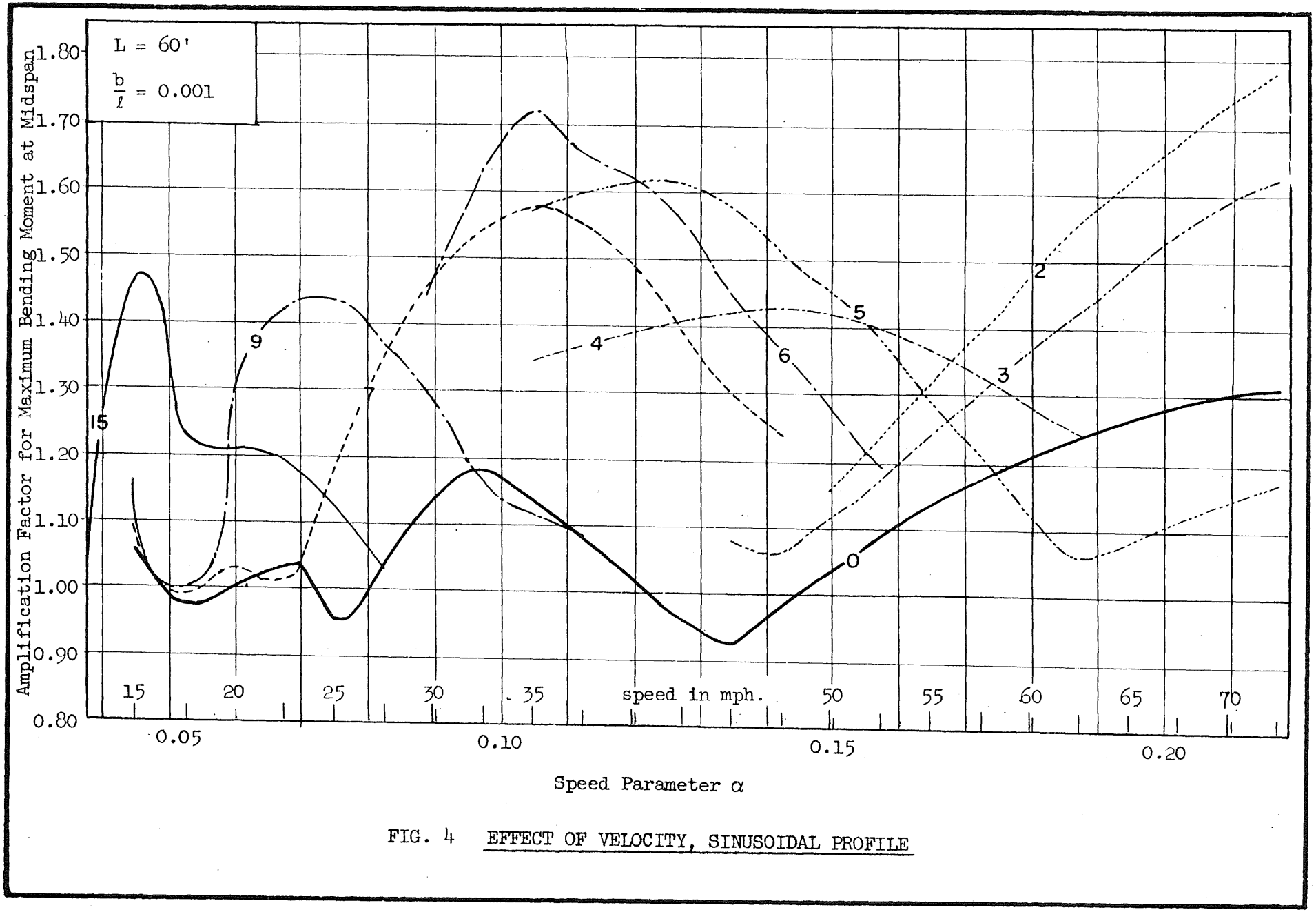

FIG. 4 EFFECT OF VELOCITY, SINUSOIDAL PROFILE

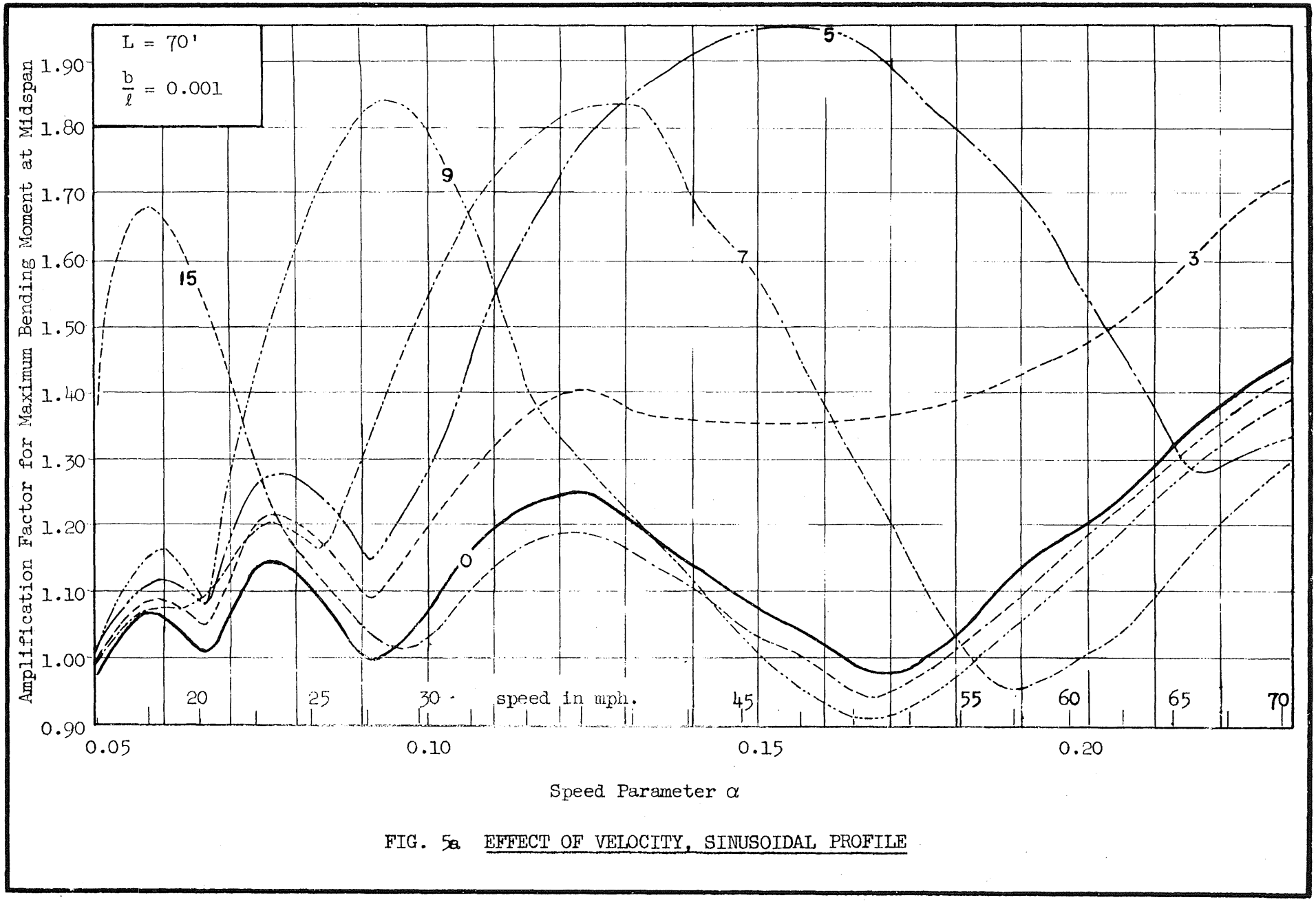

FIG. 5a EFFECT OF VELOCITY, SINUSOIDAL PROFILE

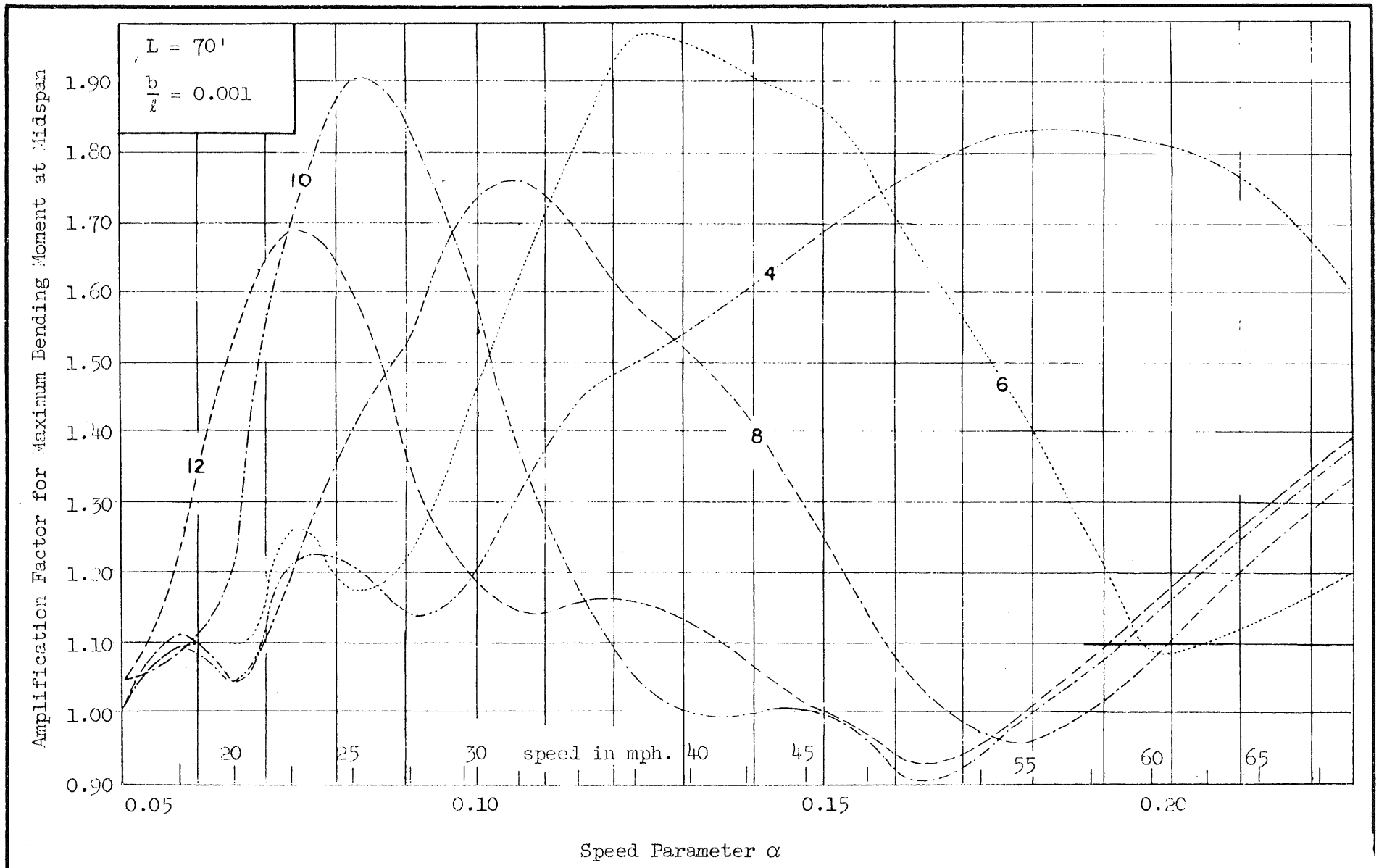

FIG. 5b EFFECT OF VELOCITY, SINUSOIDAL PROFILE

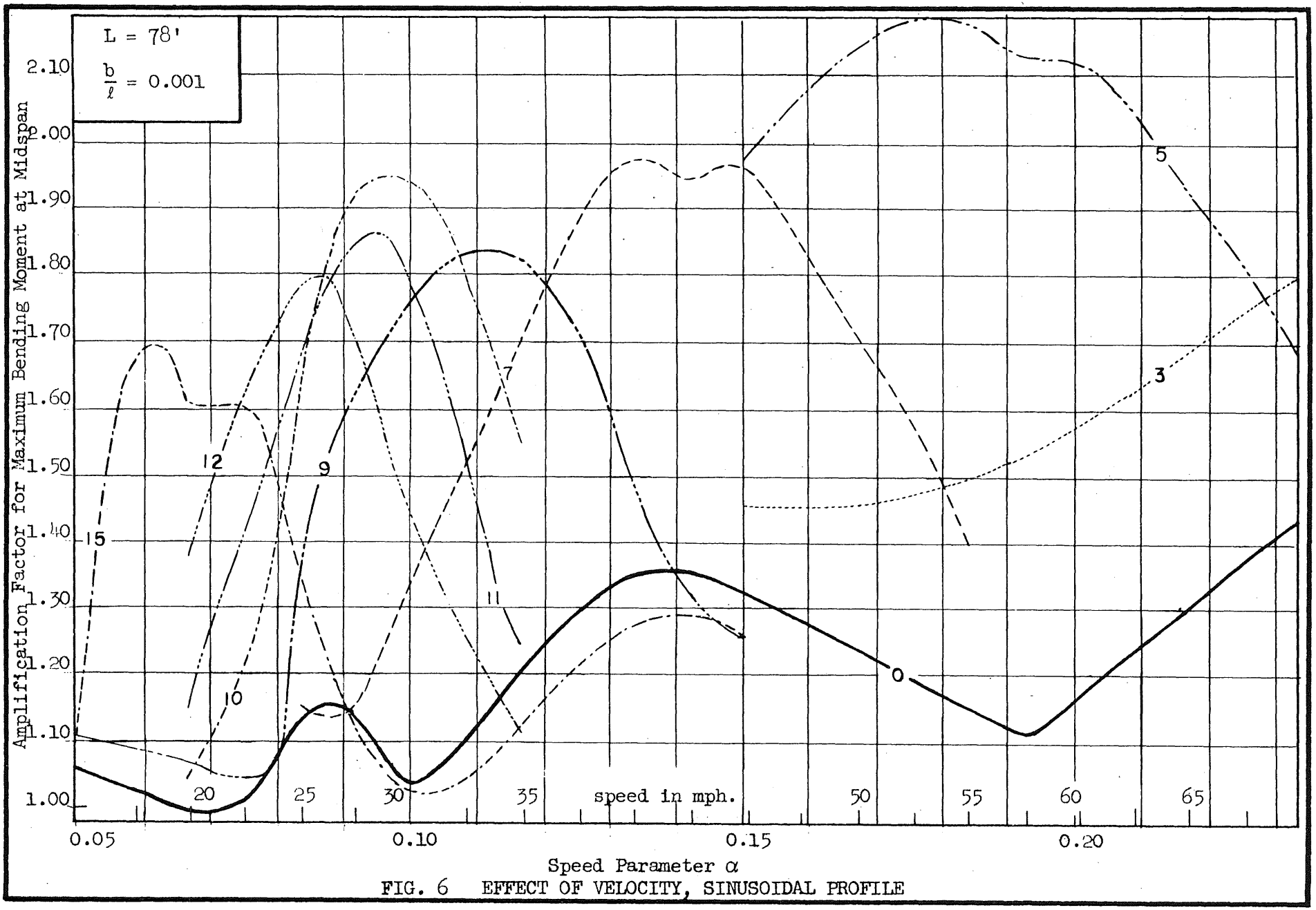

FIG. 6 EFFECT OF VELOCITY, SINUSOIDAL PROFILE

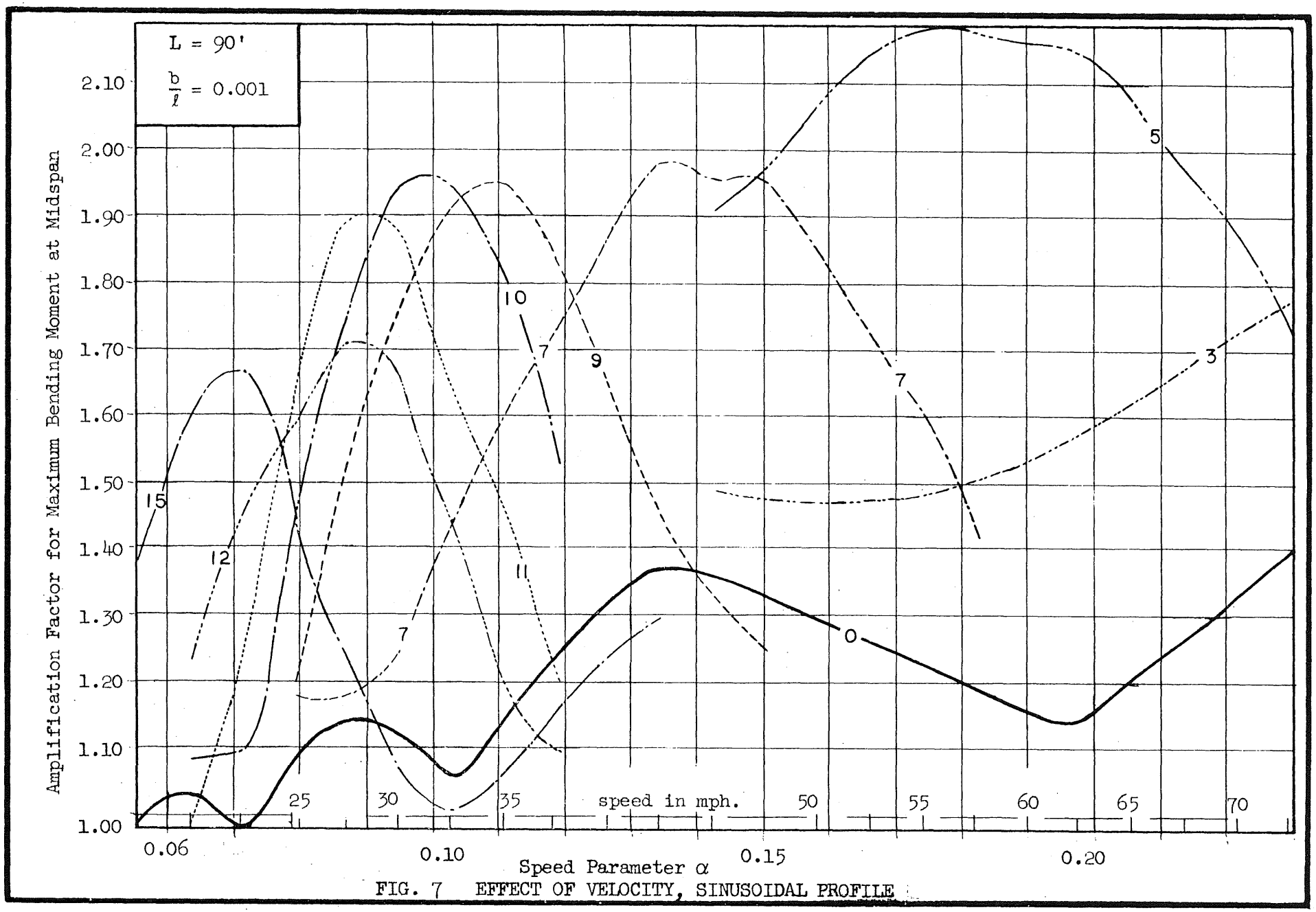

FIG. 7 EFFECT OF VELOCITY, SINUSOIDAL PROFILE

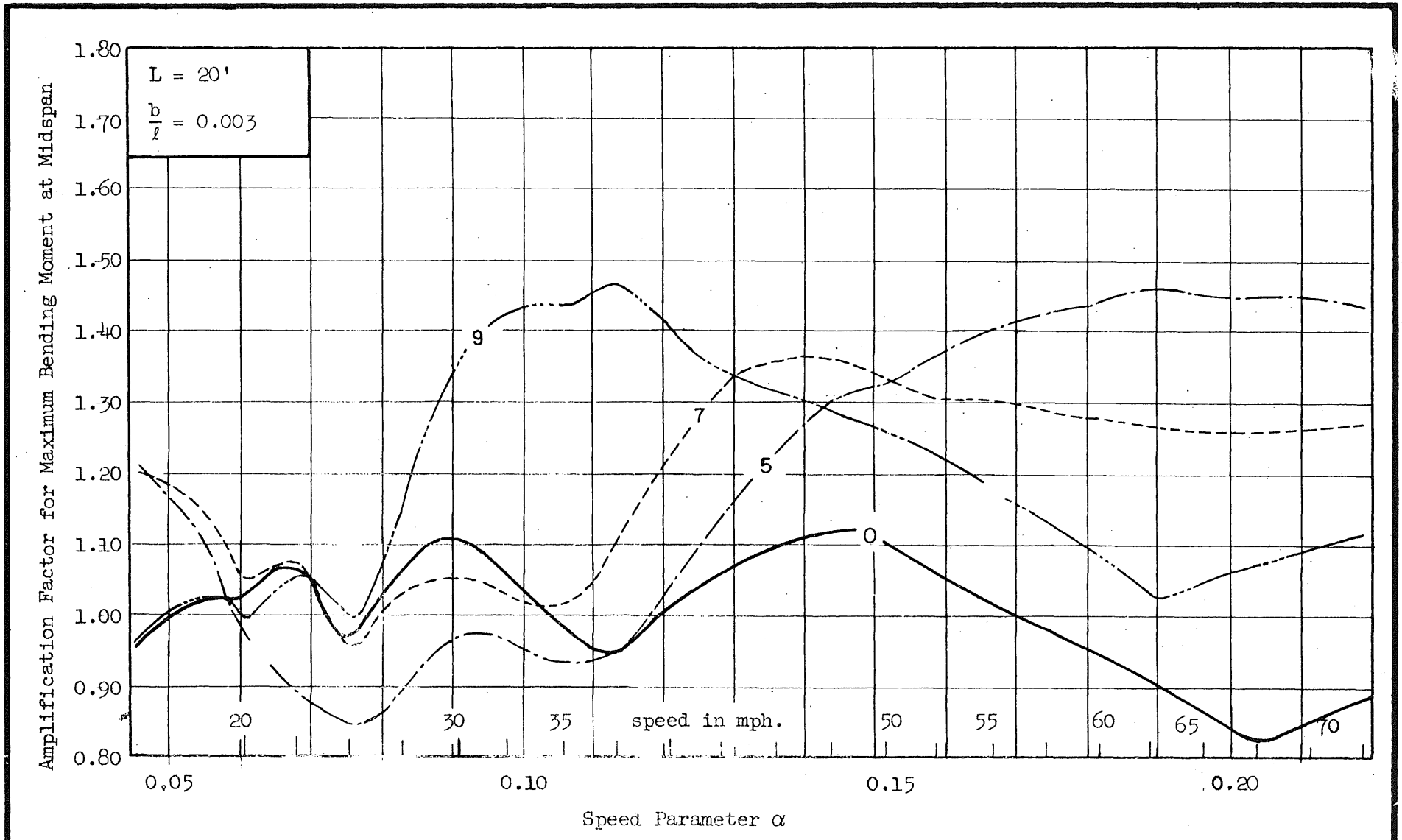

FIG. 8 EFFECT OF VELOCITY, SINUSOIDAL PROFILE

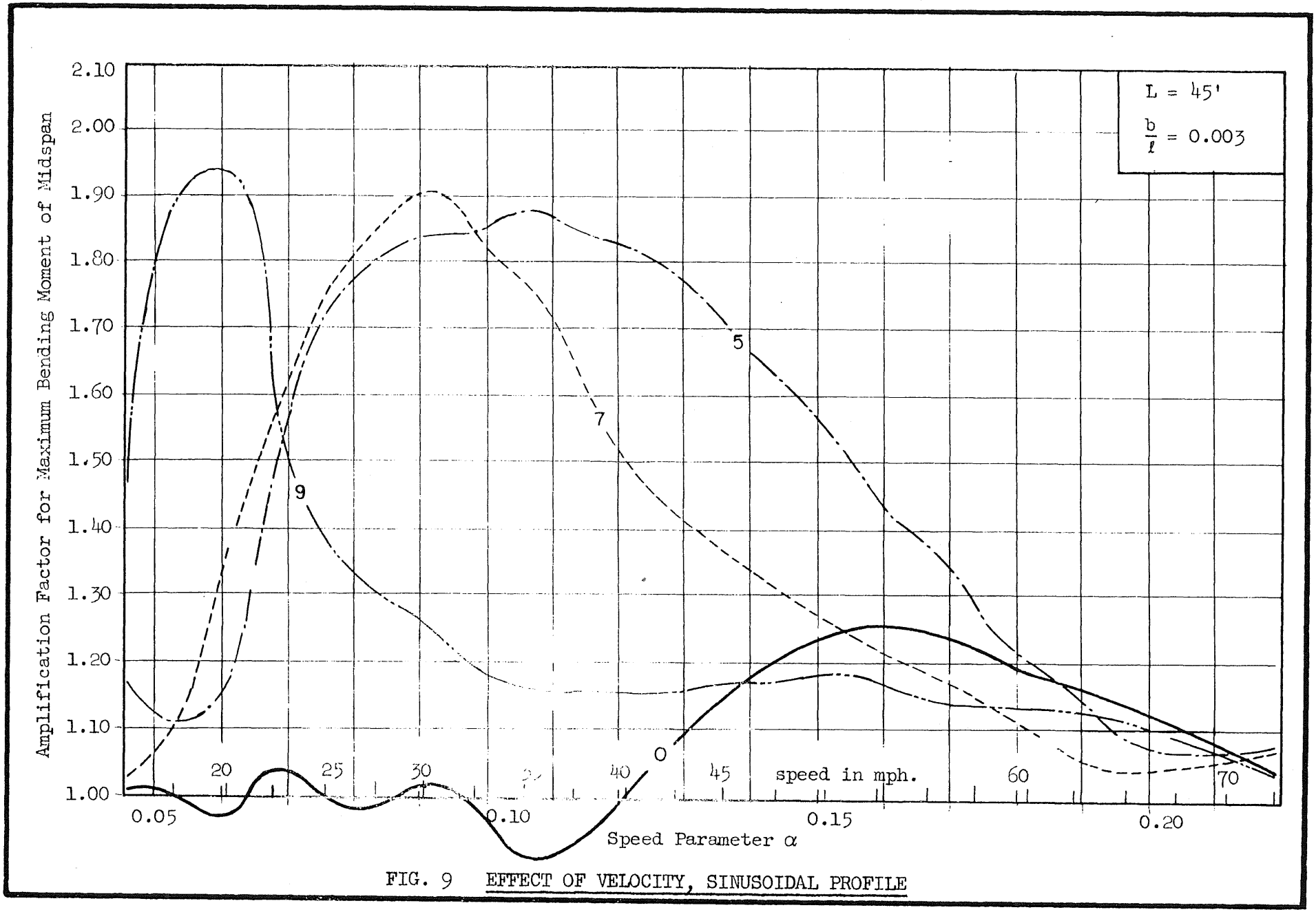

FIG. 9 EFFECT OF VELOCITY, SINUSOIDAL PROFILE

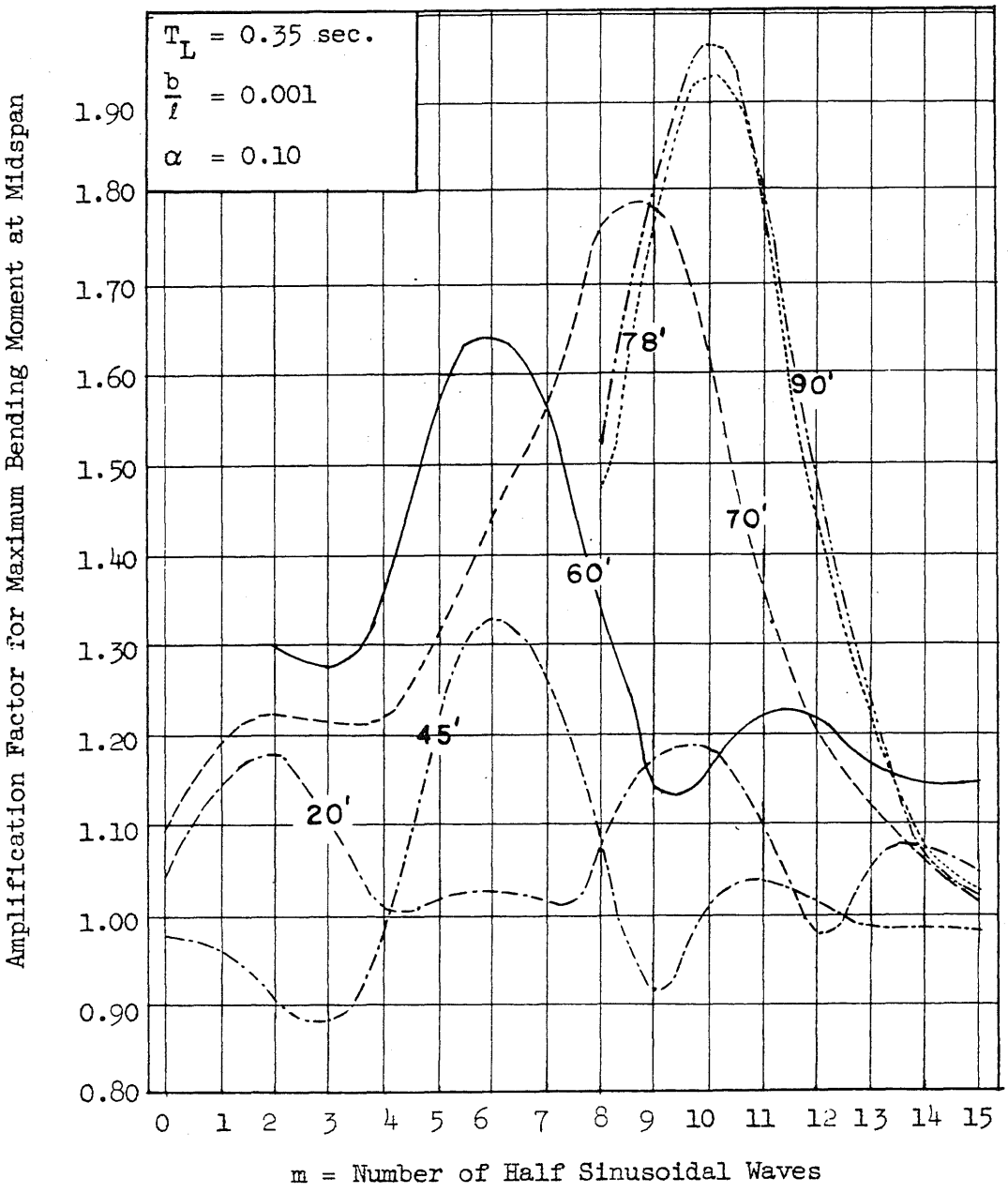

FIG. 10 EFFECT OF NUMBER OF HALF SINE WAVES

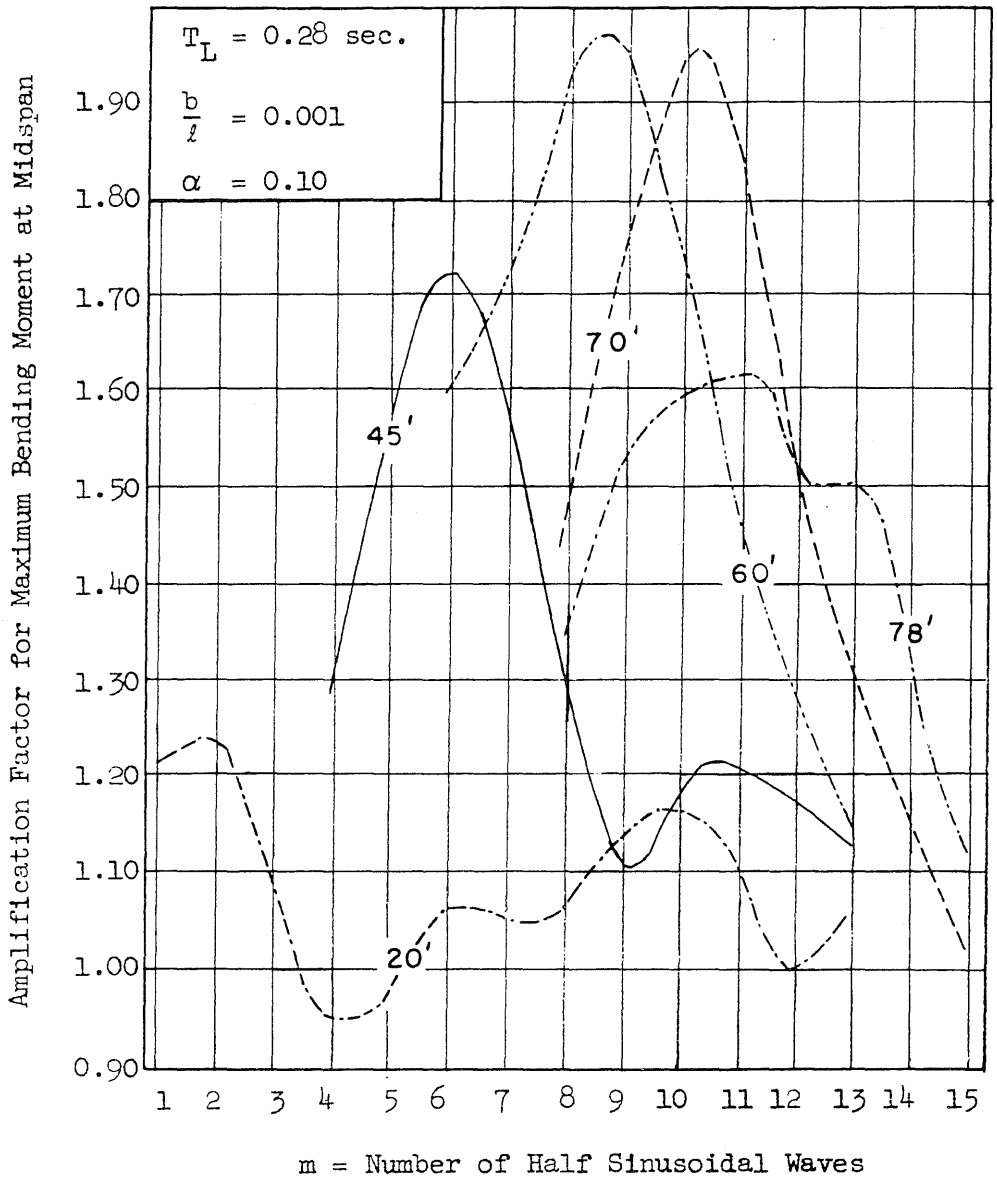

FIG. 11 EFFECT OF NUMBER OF HALF SINE WAVES

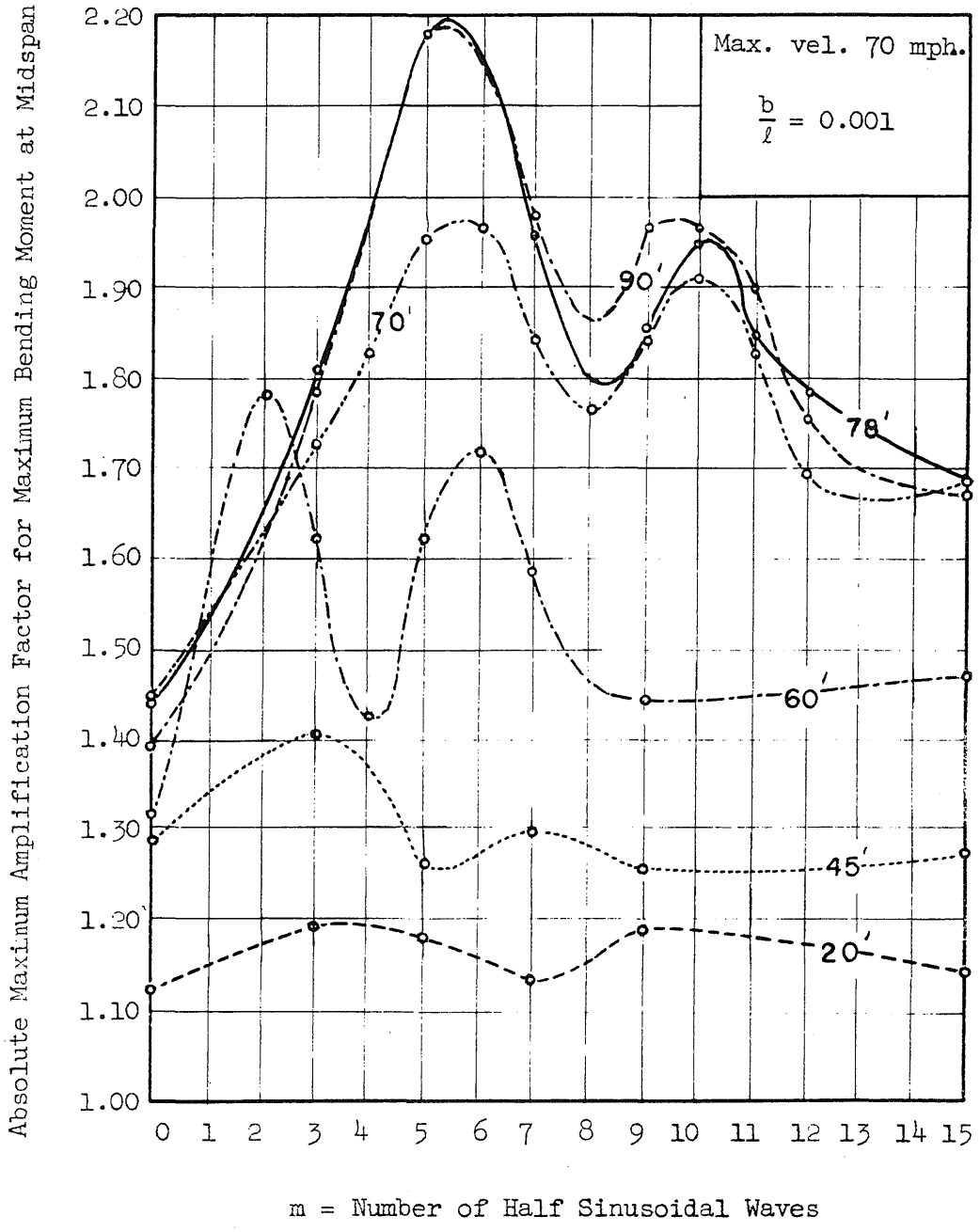

FIG. 12a ABSOLUTE MAXIMUM MOMENT AT MIDSPAN, SINUSOIDAL PROFILE

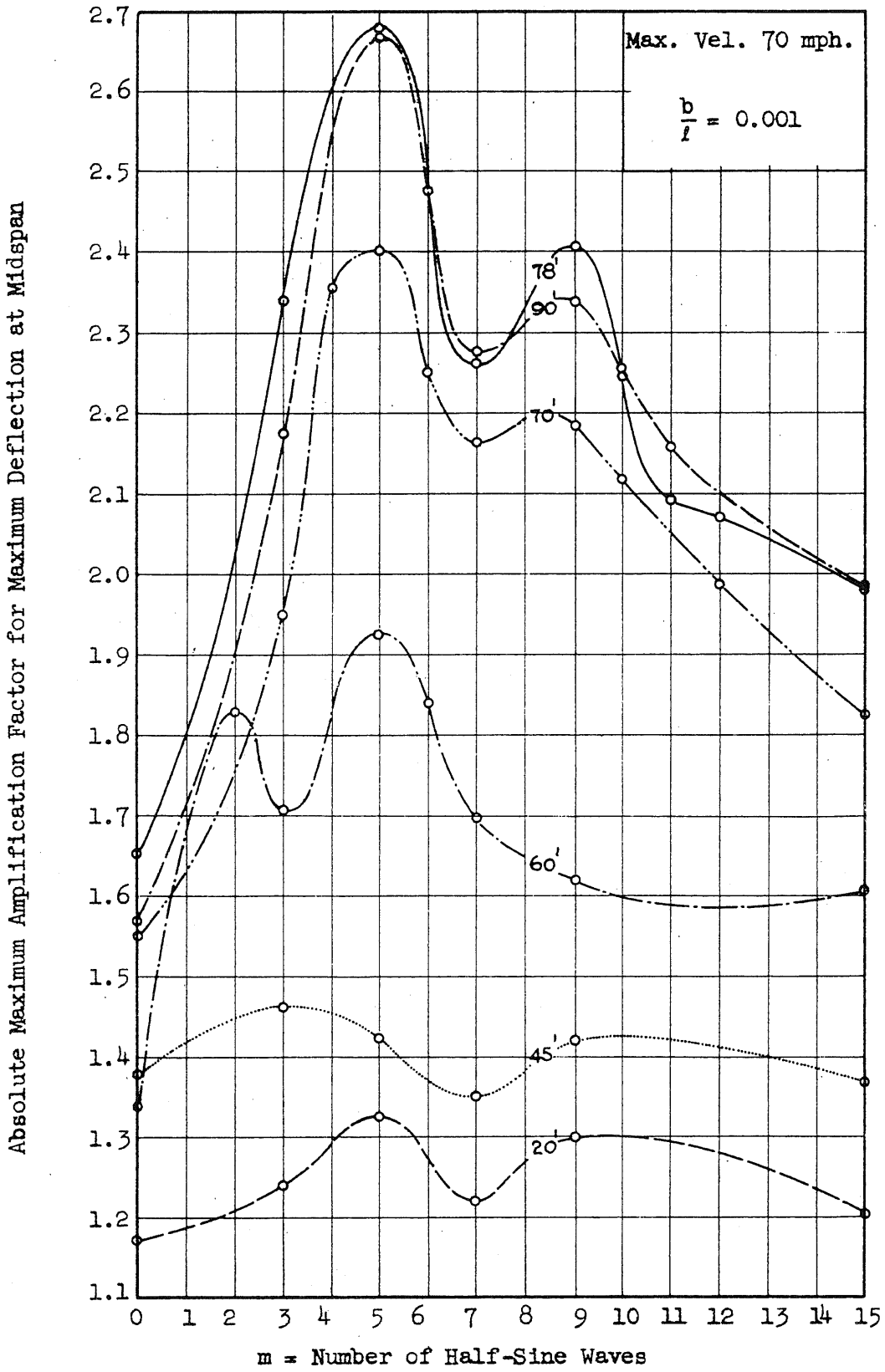

FIG. 12b ABSOLUTE MAXIMUM DEFLECTION AT MIDSPAN--SINUSOIDAL PROFILE

Maximum Velocity 70 mph.

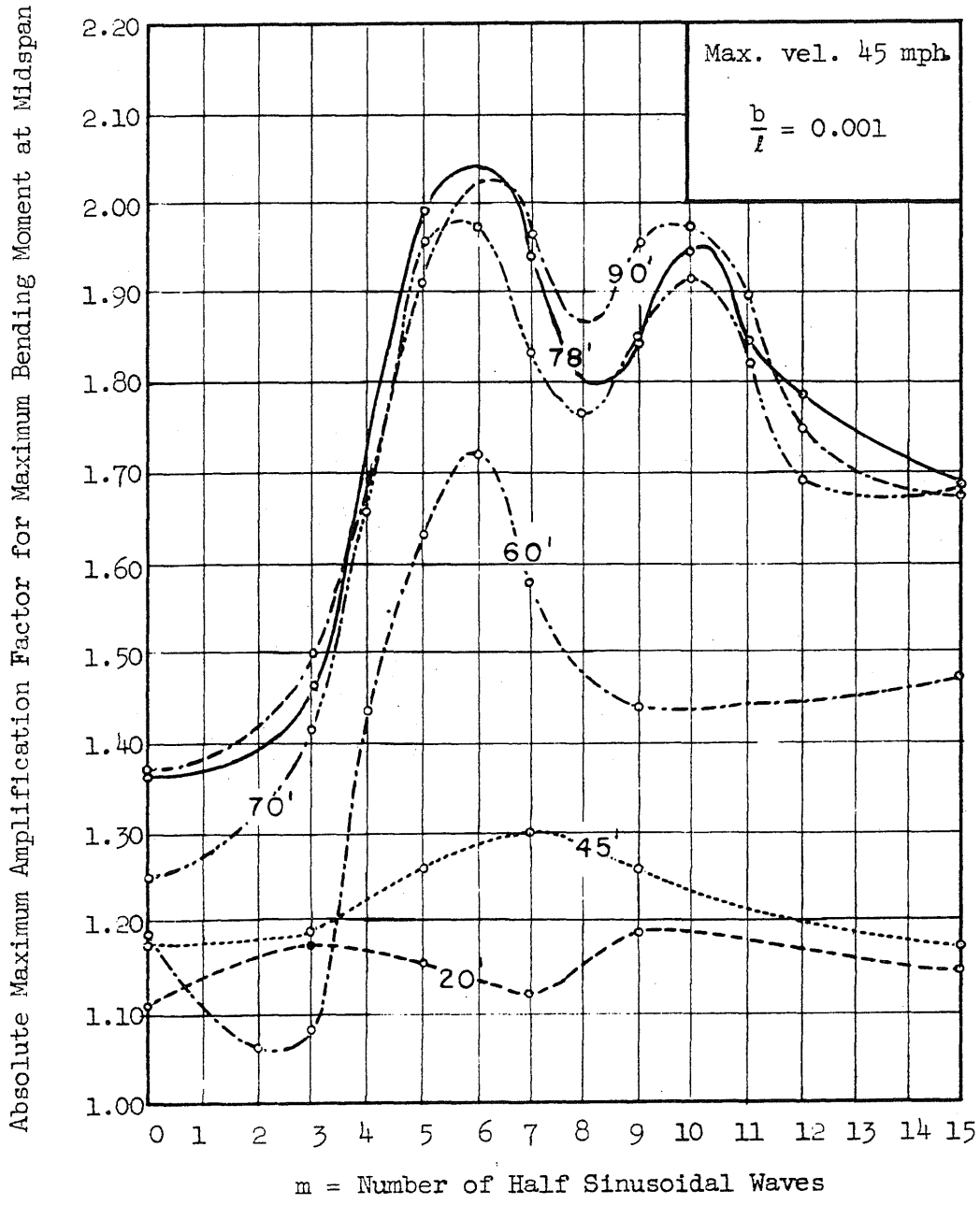

FIG. 13a ABSOLUTE MAXIMUM MOMENT AT MIDSPAN, SINUSOIDAL PROFILE

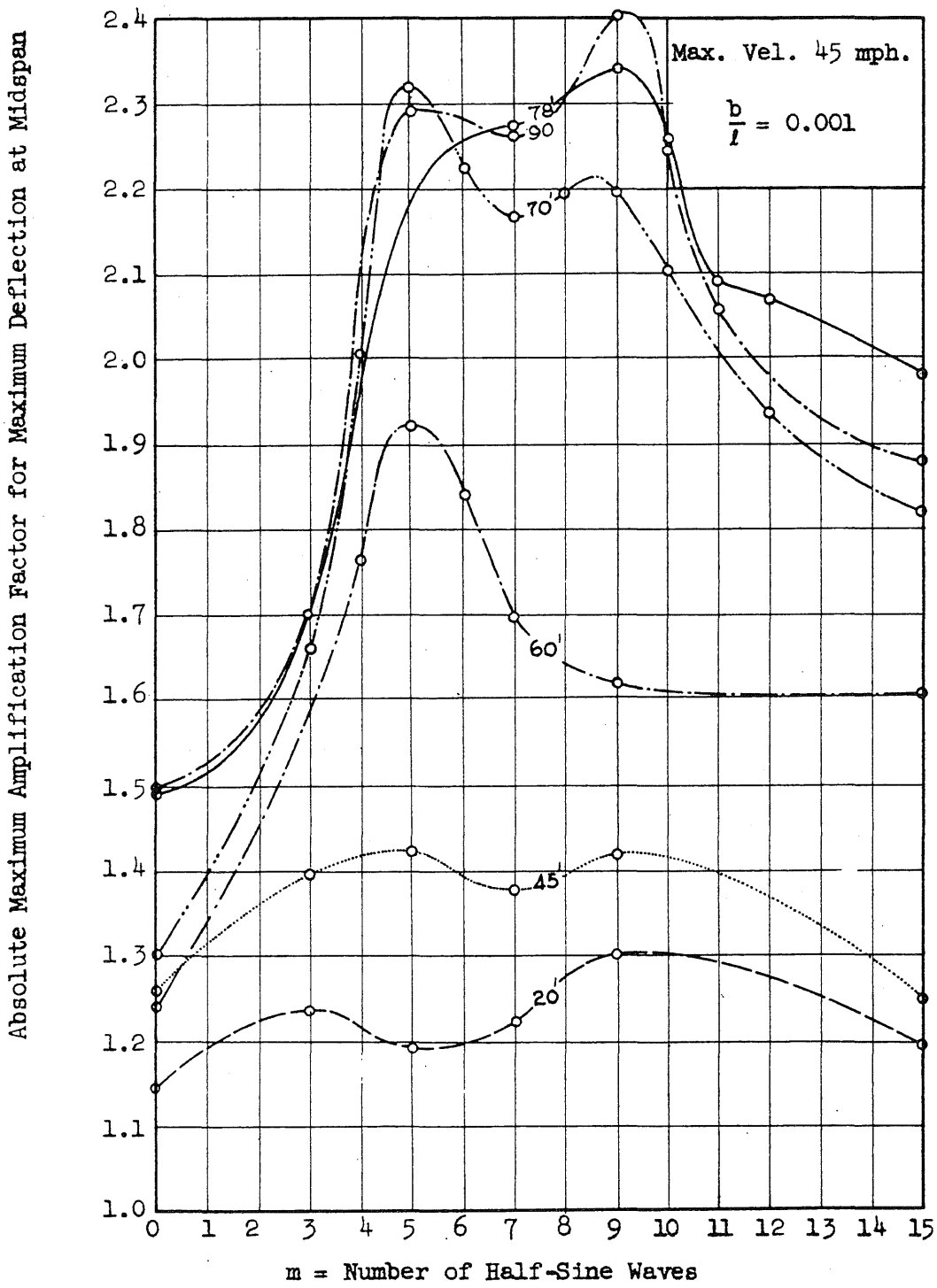

FIG. 13b ABSOLUTE MAXIMUM DEFLECTION AT MIDSPAN--SINUSOIDAL PROFILE

Maximum Velocity 45 mph.

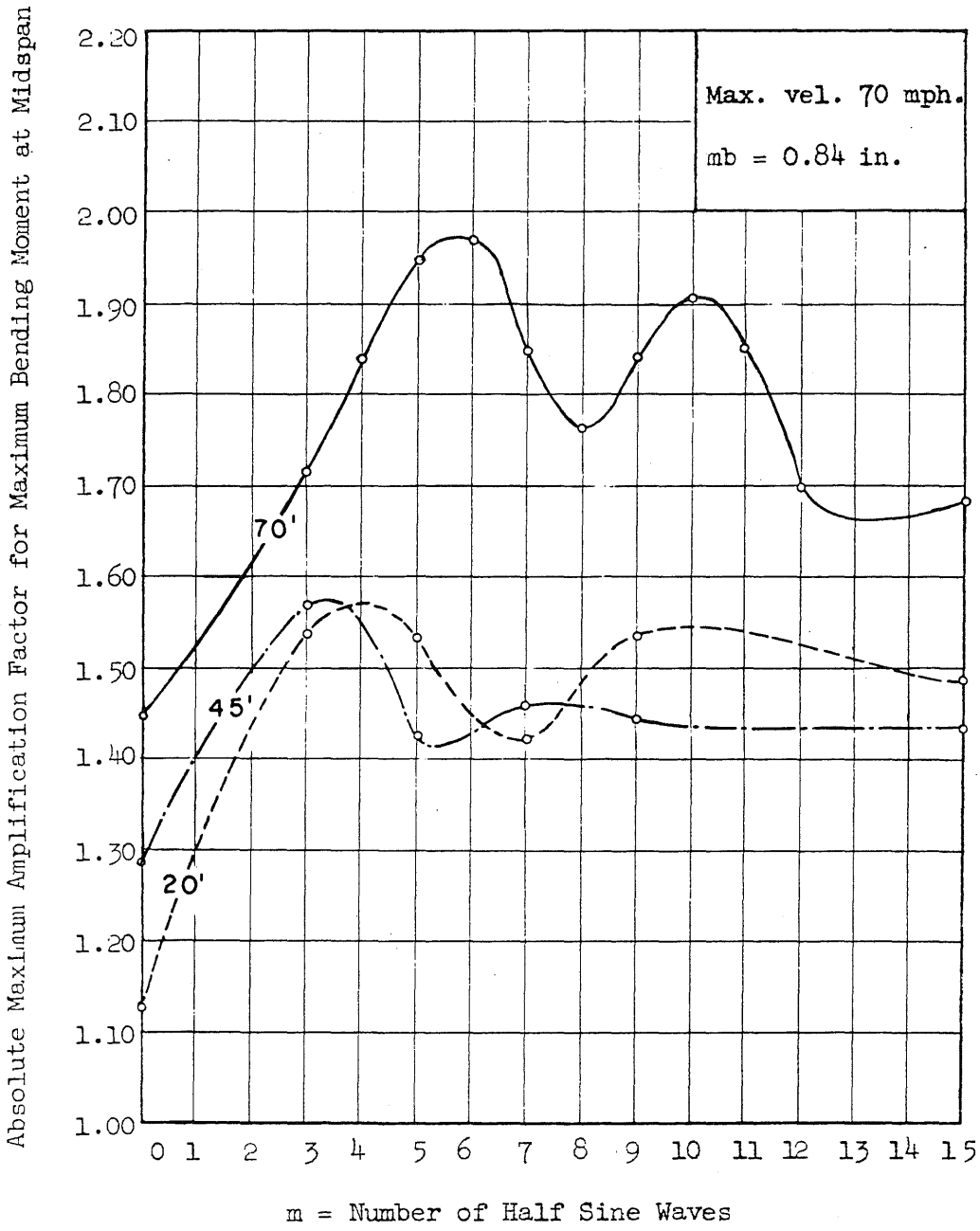

FIG. 14 ABSOLUTE MAXIMUM RESPONSE AT MIDSPAN, SINUSOIDAL PROFILE

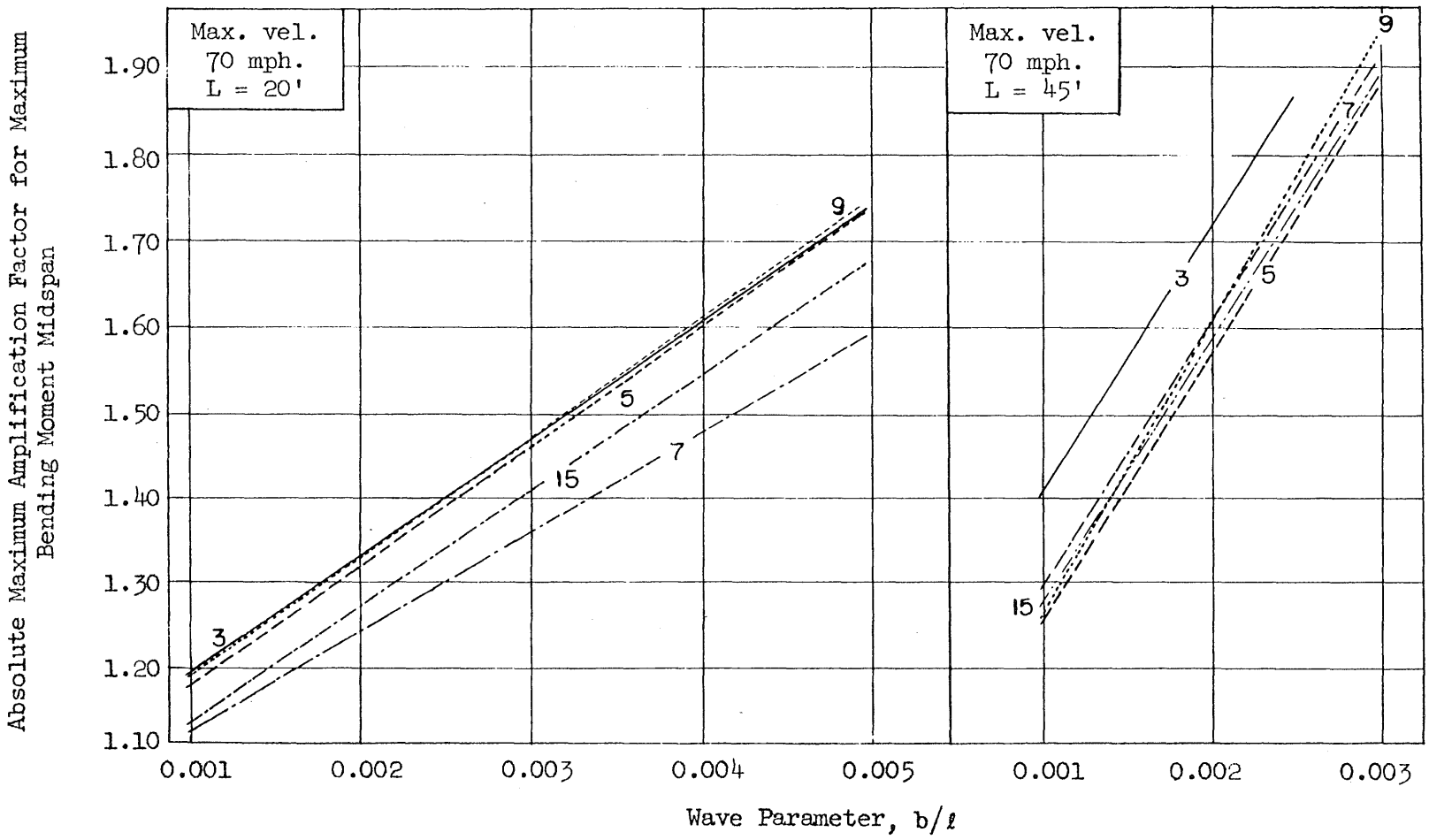

FIG. 15 EFFECT OF WAVE PARAMETER

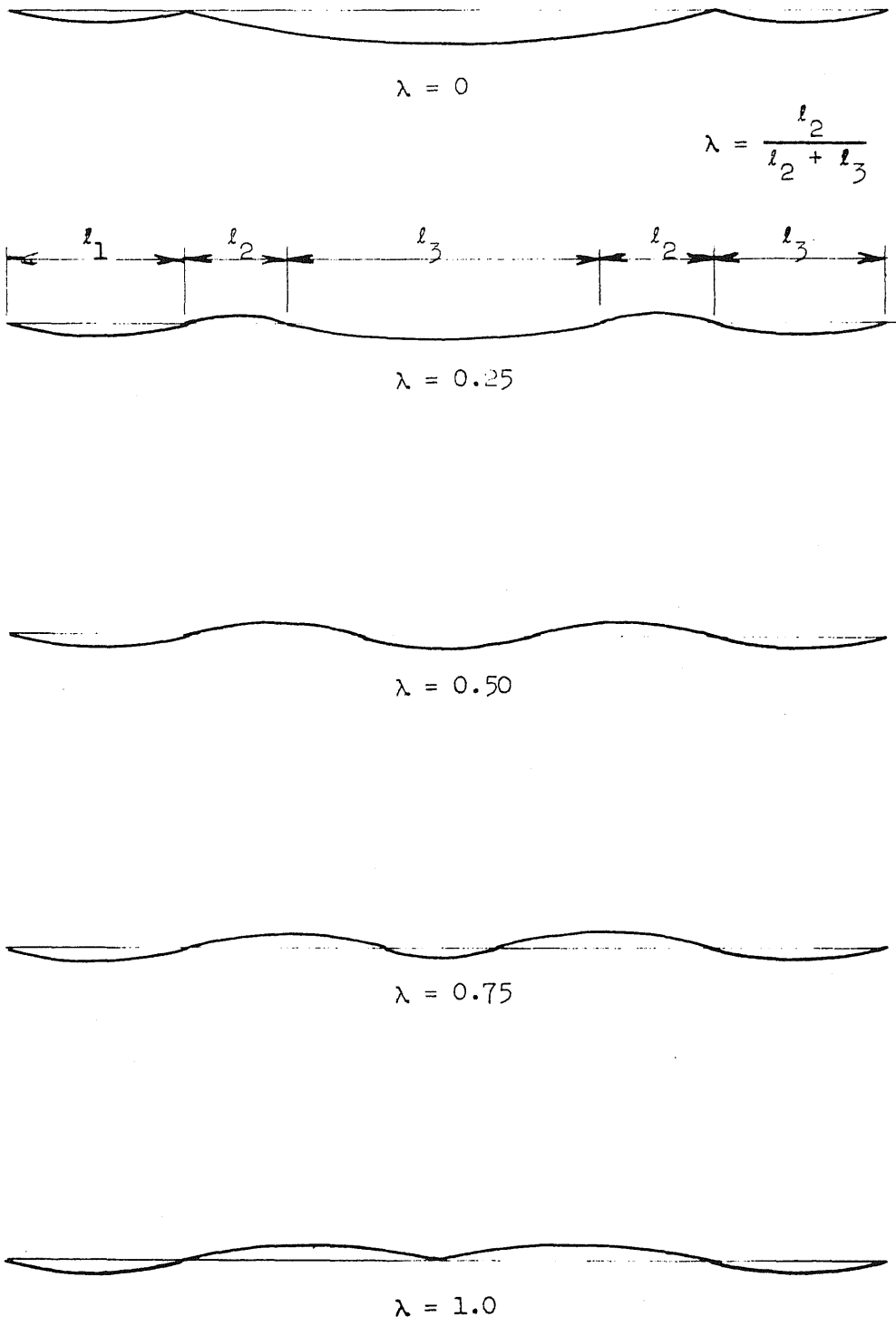

FIG. 16 SURFACE CONDITIONS CORRESPONDING TO DIFFERENT VALUES OF λ

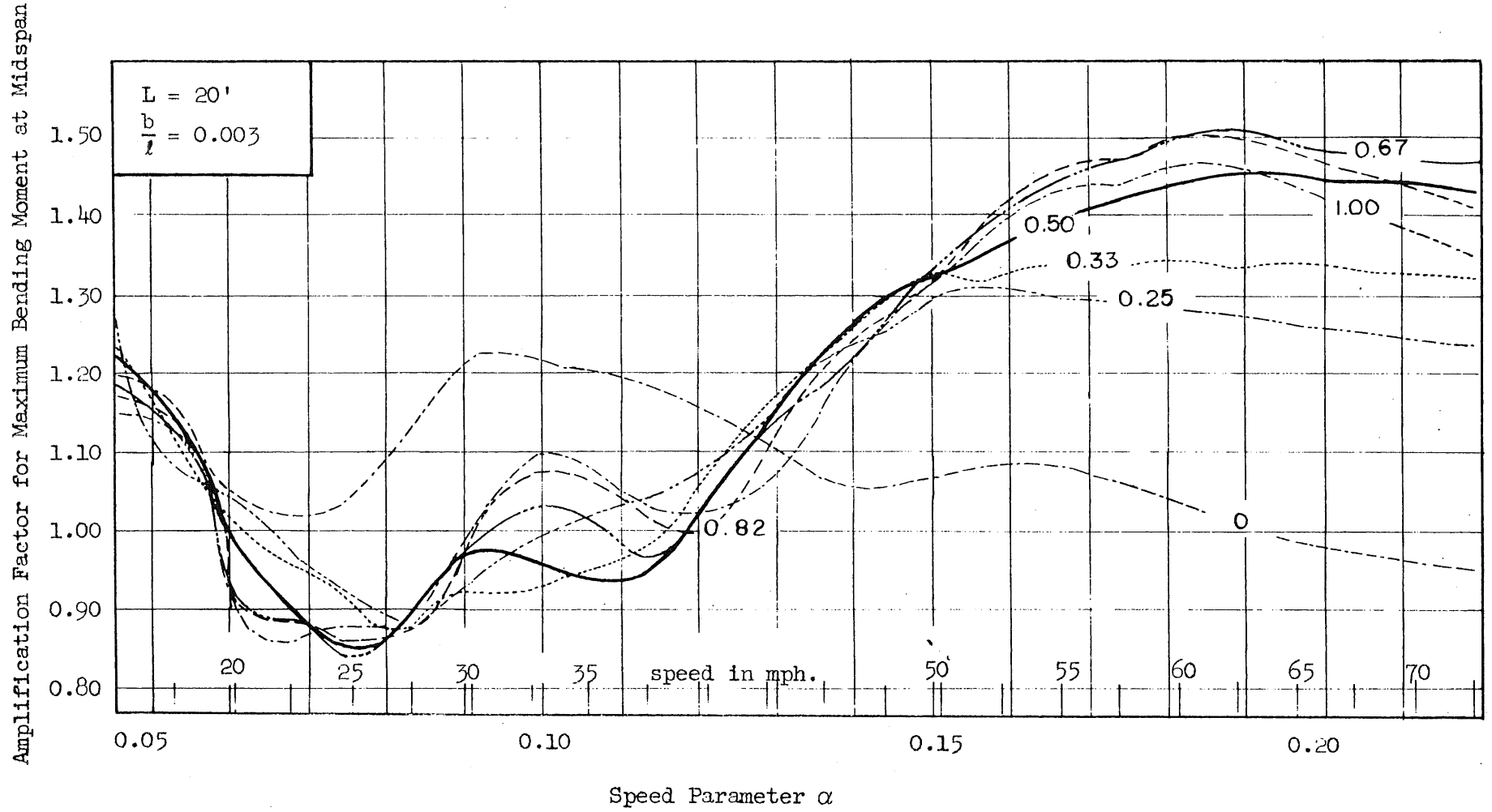

FIG. 17 EFFECT OF VELOCITY, SEMI-SYSTEMATIC PROFILE

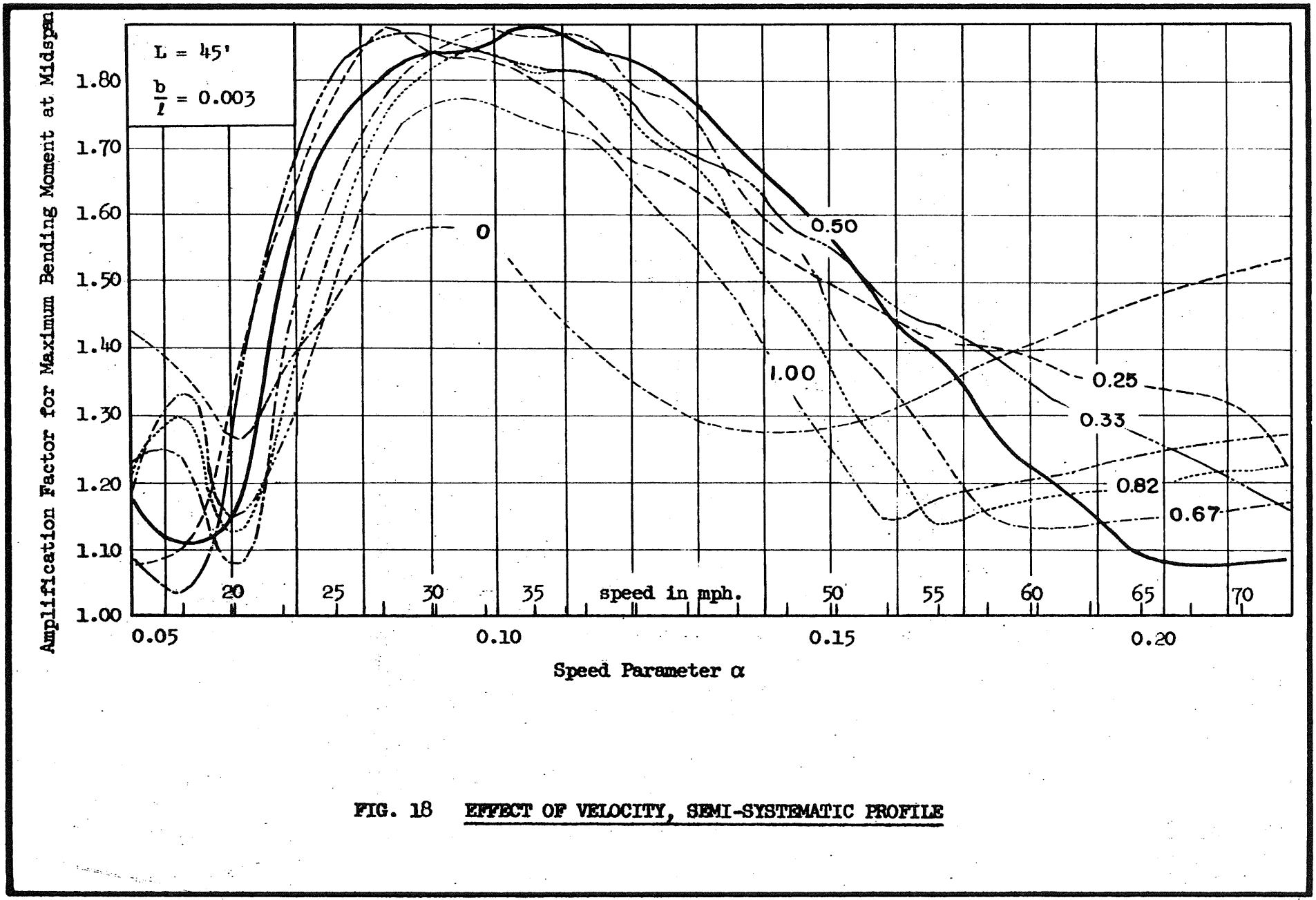

FIG. 18 EFFECT OF VELOCITY, SEMI-SYSTEMATIC PROFILE

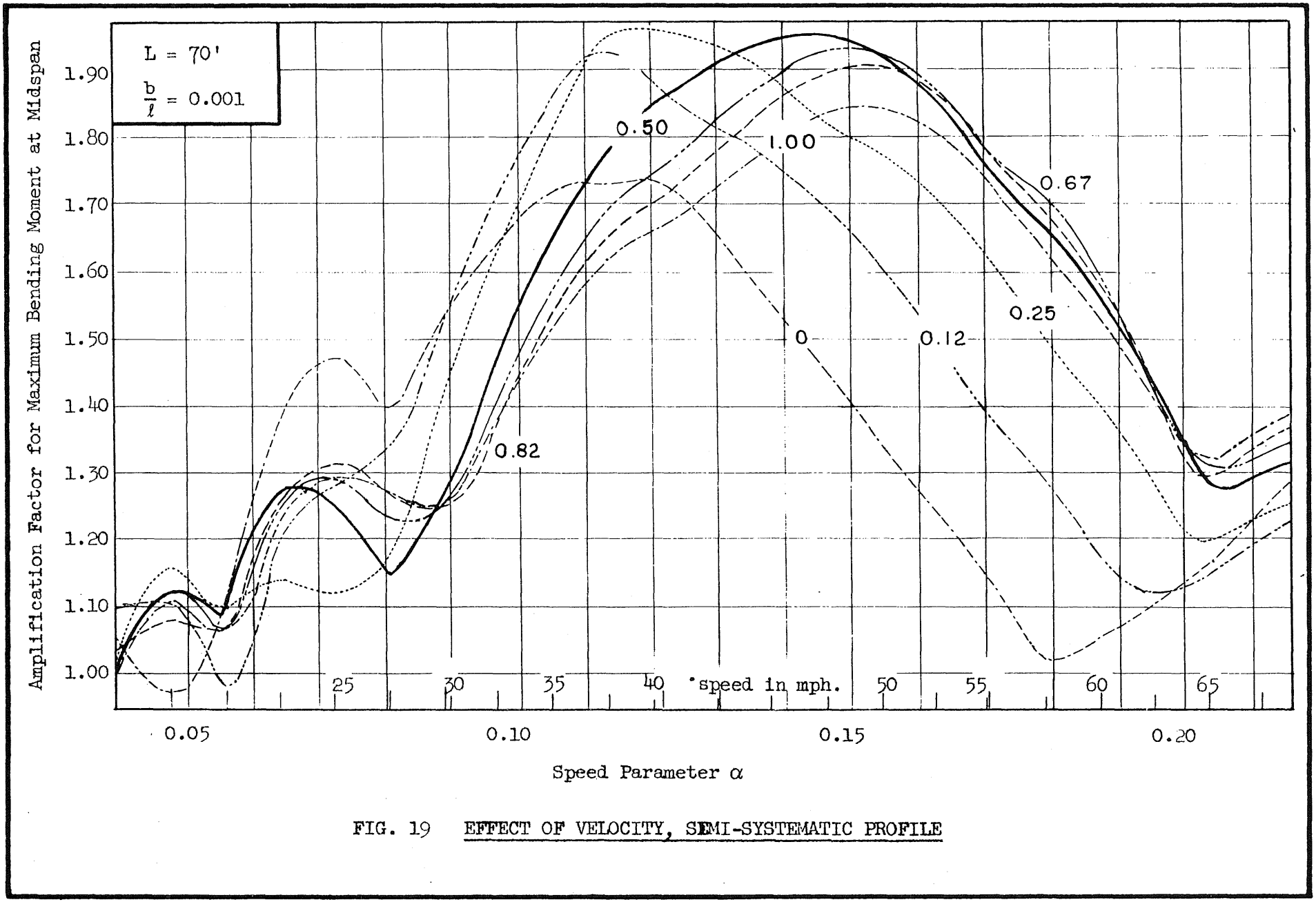

FIG. 19 EFFECT OF VELOCITY, SEMI-SYSTEMATIC PROFILE

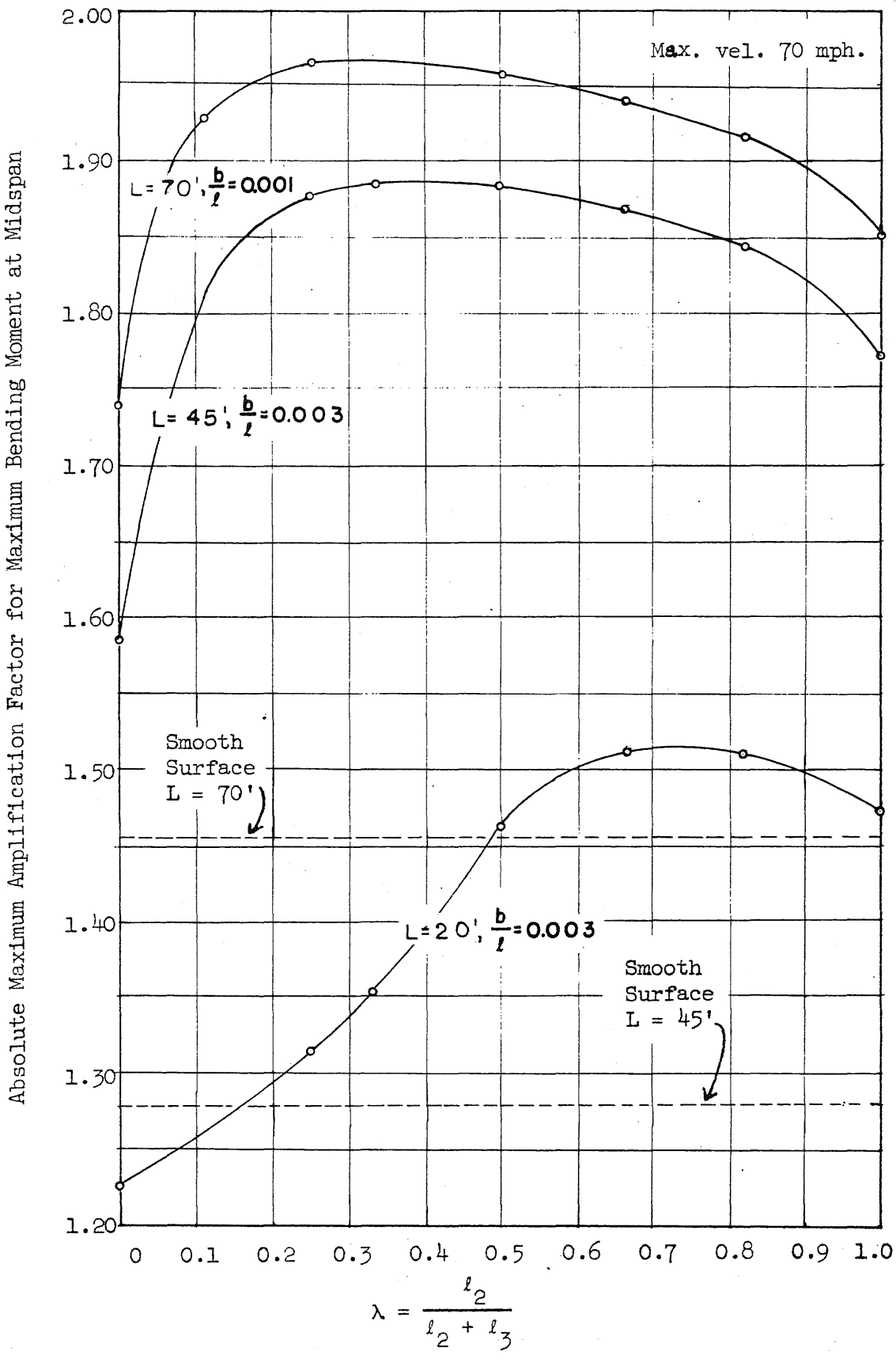

FIG. 20a ABSOLUTE MAXIMUM MOMENT AT MIDSPAN, SEMI-SYSTEMATIC PROFILE

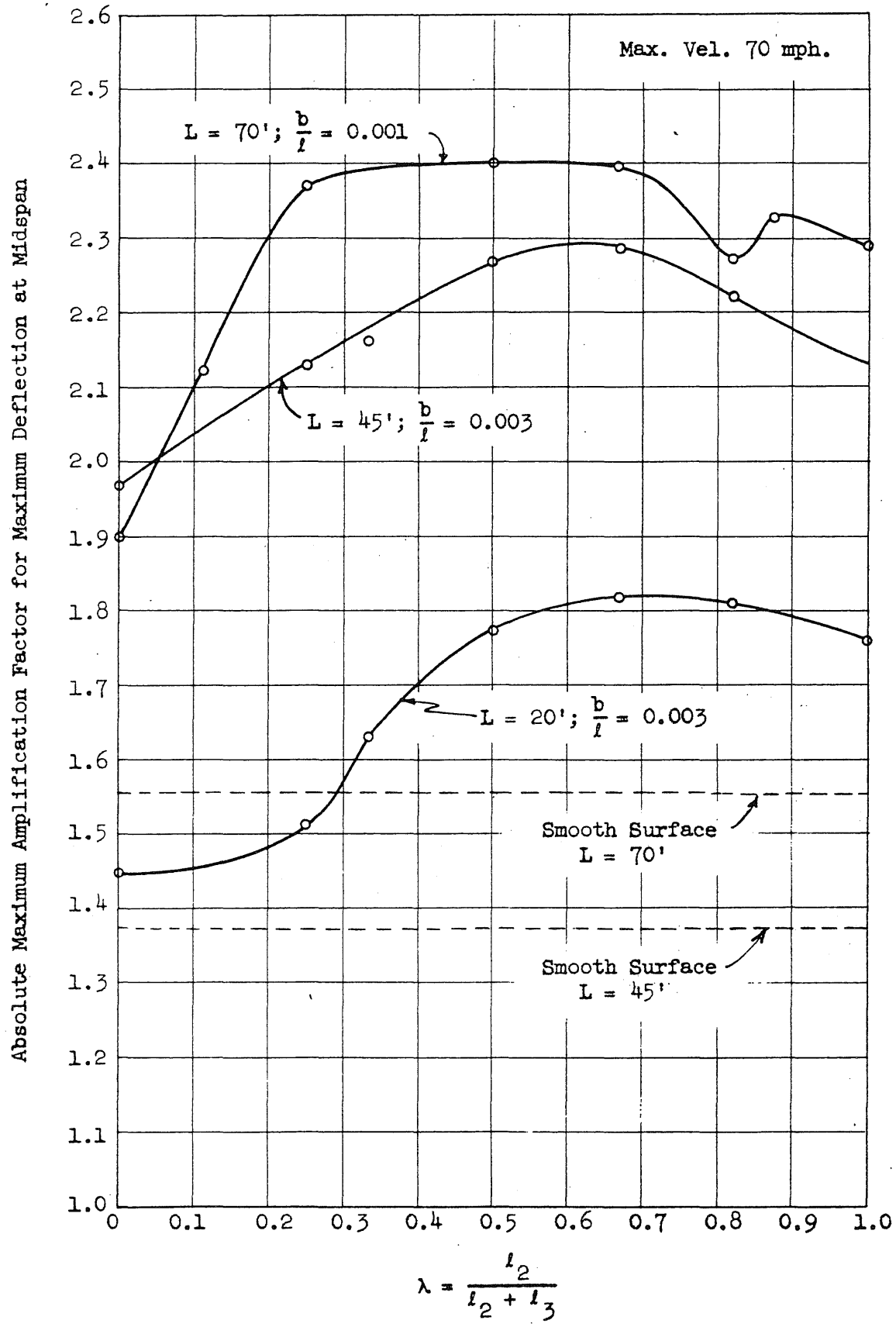

FIG. 20b ABSOLUTE MAXIMUM DEFLECTION AT MIDSPAN--EFFECT OF SEMI-SYSTEMATIC PROFILE

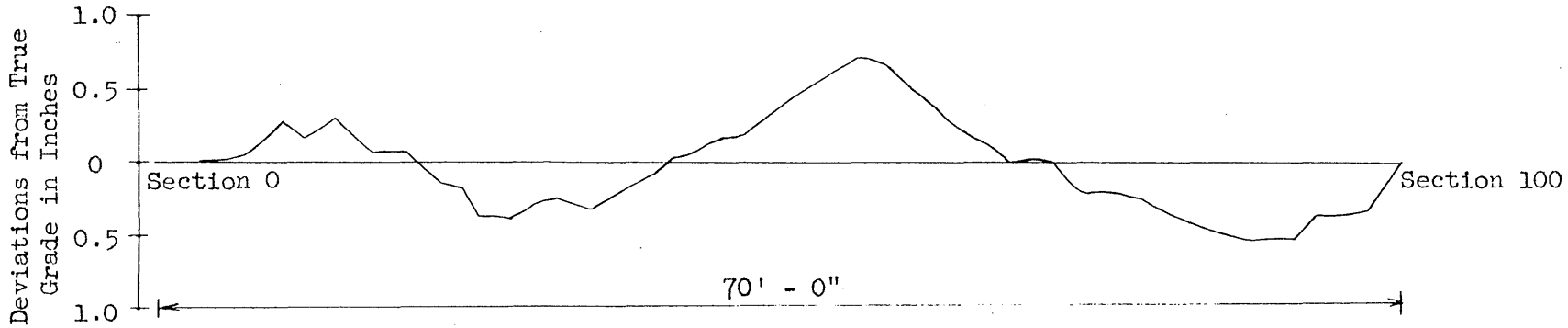

Section	Deviation (in.)	Section	Deviation (in.)	Section	Deviation (in.)	Section	Deviation (in.)	Section	Deviation (in.)
0	0.000	21	0.000	42	-0.012	63	-0.324	84	+0.456
1	0.000	22	+0.060	43	-0.036	64	-0.240	85	+0.480
2	0.000	23	+0.144	44	-0.108	65	-0.204	86	+0.504
3	0.000	24	+0.144	45	-0.132	66	-0.144	87	+0.516
4	0.000	25	+0.240	46	-0.168	67	-0.120	88	+0.504
5	0.000	26	+0.360	47	-0.180	68	-0.048	89	+0.492
6	0.000	27	+0.372	48	-0.252	69	0.000	90	+0.492
7	-0.048	28	+0.372	49	-0.300	70	0.000	91	+0.492
8	-0.108	29	+0.372	50	-0.360	71	0.000	92	+0.444
9	-0.180	30	+0.324	51	-0.420	72	+0.024	93	+0.372
10	-0.252	31	+0.252	52	-0.456	73	+0.120	94	+0.372
11	-0.192	32	+0.252	53	-0.504	74	+0.204	95	+0.372
12	-0.144	33	+0.300	54	-0.564	75	+0.216	96	+0.360
13	-0.228	34	+0.336	55	-0.612	76	+0.216	97	+0.360
14	-0.252	35	+0.324	56	-0.696	77	+0.216	98	+0.240
15	-0.240	36	+0.252	57	-0.696	78	+0.240	99	+0.120
16	-0.156	37	+0.228	58	-0.696	79	+0.276	100	0.000
17	-0.108	38	+0.180	59	-0.660	80	+0.312		
18	-0.060	39	+0.132	60	-0.588	81	+0.348		
19	-0.060	40	+0.096	61	-0.480	82	+0.396		
20	-0.072	41	0.000	62	-0.420	83	+0.444		

FIG. 21 PORTION OF NORTH DILLARD BRIDGE PROFILE

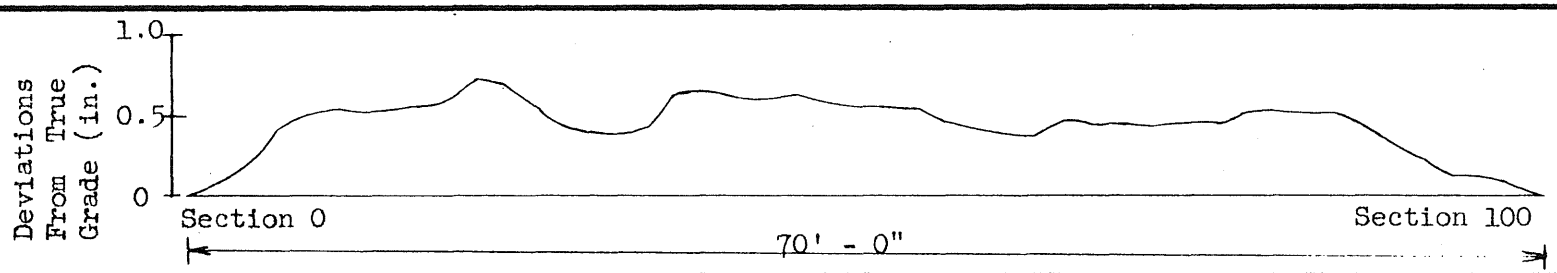

Section	Deviation (in.)	Section	Deviation (in.)	Section	Deviation (in.)	Section	Deviation (in.)	Section	Deviation (in.)
0	0.000	21	-0.708	42	-0.576	63	-0.384	84	-0.492
1	-0.024	22	-0.720	43	-0.588	64	-0.456	85	-0.492
2	-0.060	23	-0.708	44	-0.600	65	-0.468	86	-0.480
3	-0.096	24	-0.660	45	-0.612	66	-0.468	87	-0.456
4	-0.132	25	-0.600	46	-0.588	67	-0.444	88	-0.372
5	-0.192	26	-0.552	47	-0.576	68	-0.444	89	-0.336
6	-0.300	27	-0.468	48	-0.564	69	-0.456	90	-0.264
7	-0.420	28	-0.420	49	-0.552	70	-0.432	91	-0.240
8	-0.468	29	-0.384	50	-0.540	71	-0.432	92	-0.180
9	-0.492	30	-0.384	51	-0.540	72	-0.432	93	-0.132
10	-0.492	31	-0.372	52	-0.540	73	-0.444	94	-0.120
11	-0.504	32	-0.384	53	-0.528	74	-0.456	95	-0.120
12	-0.504	33	-0.384	54	-0.516	75	-0.468	96	-0.120
13	-0.492	34	-0.432	55	-0.480	76	-0.456	97	-0.108
14	-0.492	35	-0.492	56	-0.420	77	-0.468	98	-0.072
15	-0.516	36	-0.600	57	-0.420	78	-0.492	99	-0.024
16	-0.528	37	-0.636	58	-0.396	79	-0.504	100	0.000
17	-0.552	38	-0.624	59	-0.384	80	-0.516		
18	-0.576	39	-0.624	60	-0.372	81	-0.504		
19	-0.588	40	-0.600	61	-0.360	82	-0.492		
20	-0.612	41	-0.588	62	-0.360	83	-0.492		

FIG. 22 PORTION OF MILLER'S CREEK BRIDGE PROFILE

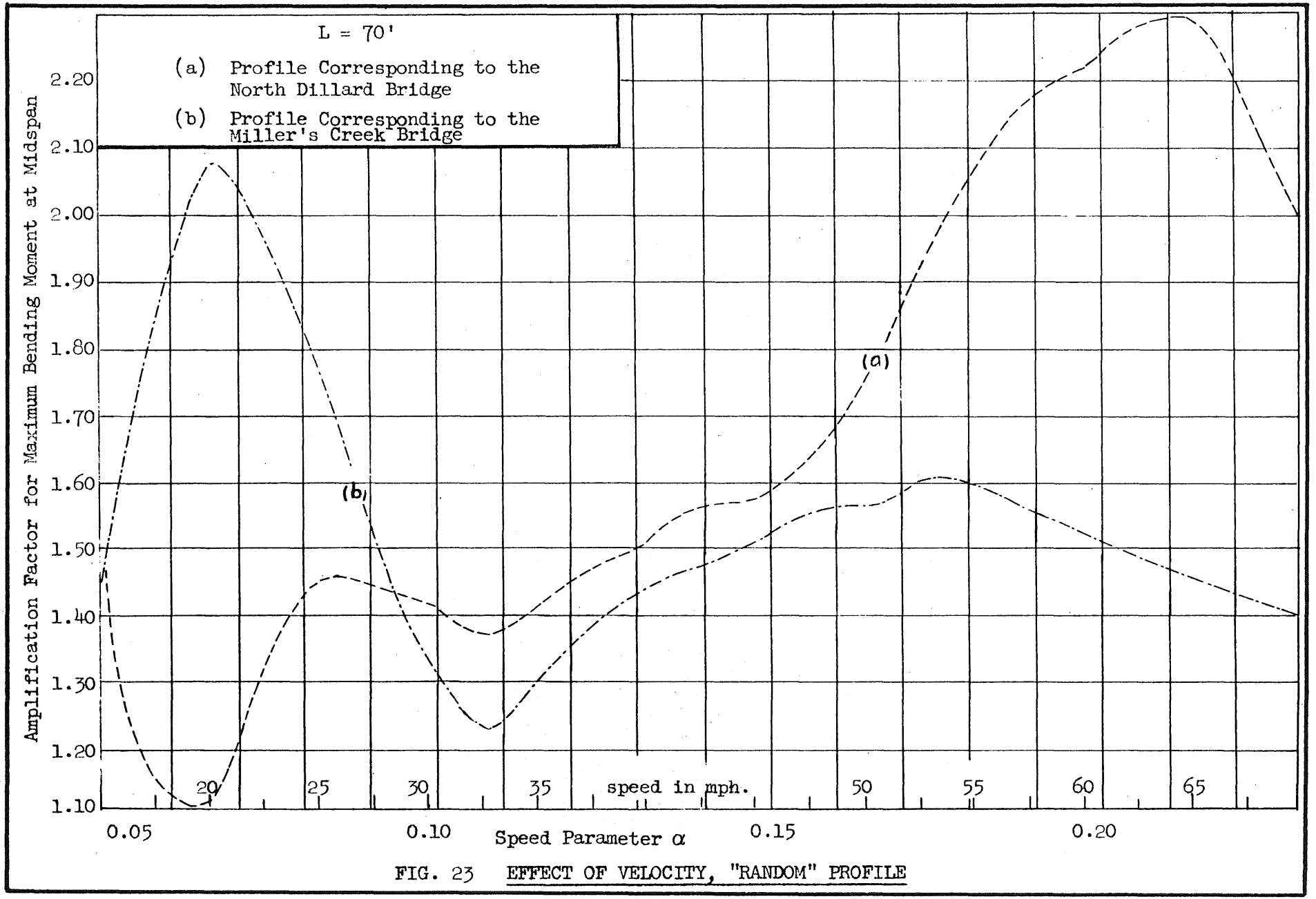

FIG. 23 EFFECT OF VELOCITY, "RANDOM" PROFILE

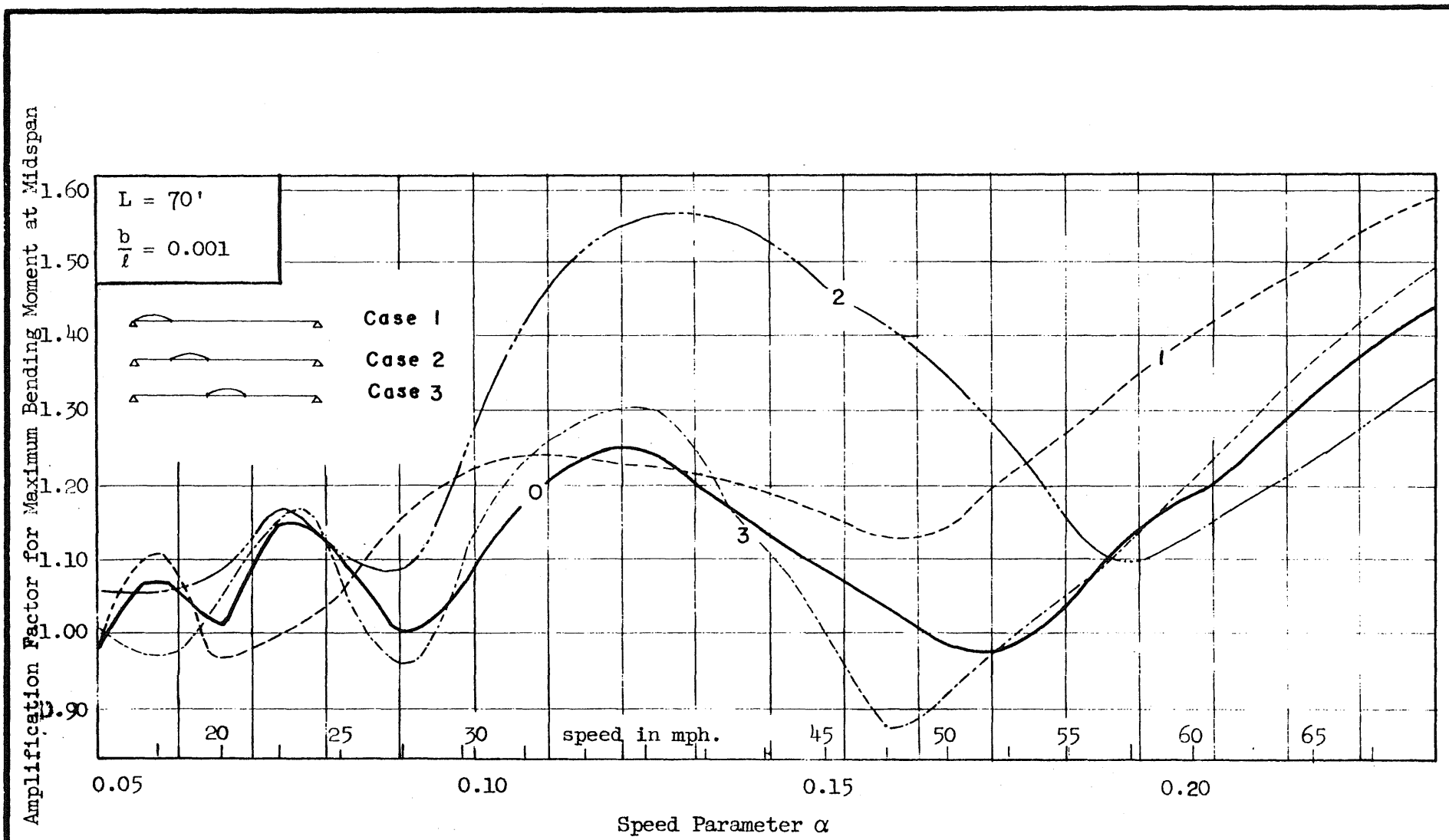

FIG. 24 EFFECT OF VELOCITY, LOCALIZED IRREGULARITY

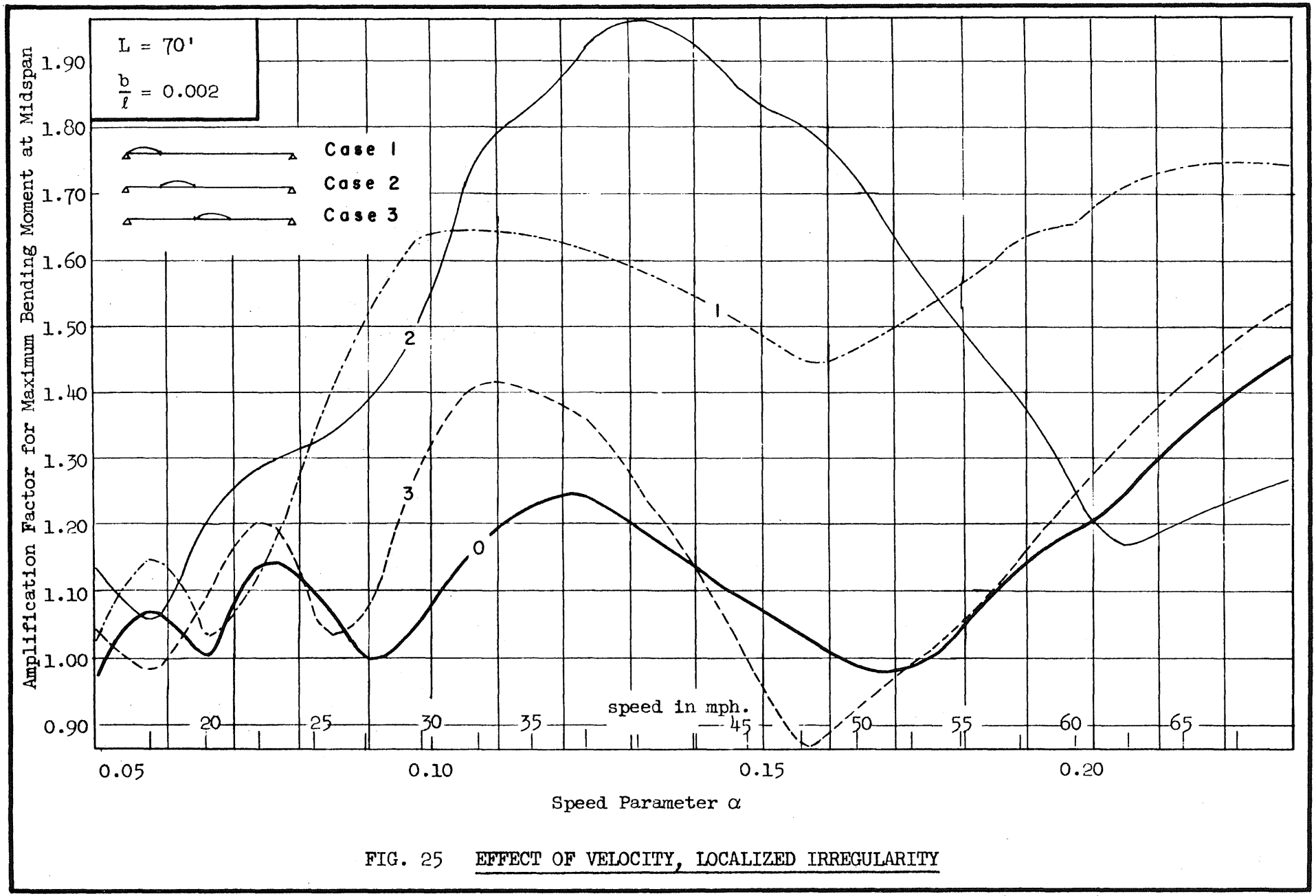

FIG. 25 EFFECT OF VELOCITY, LOCALIZED IRREGULARITY

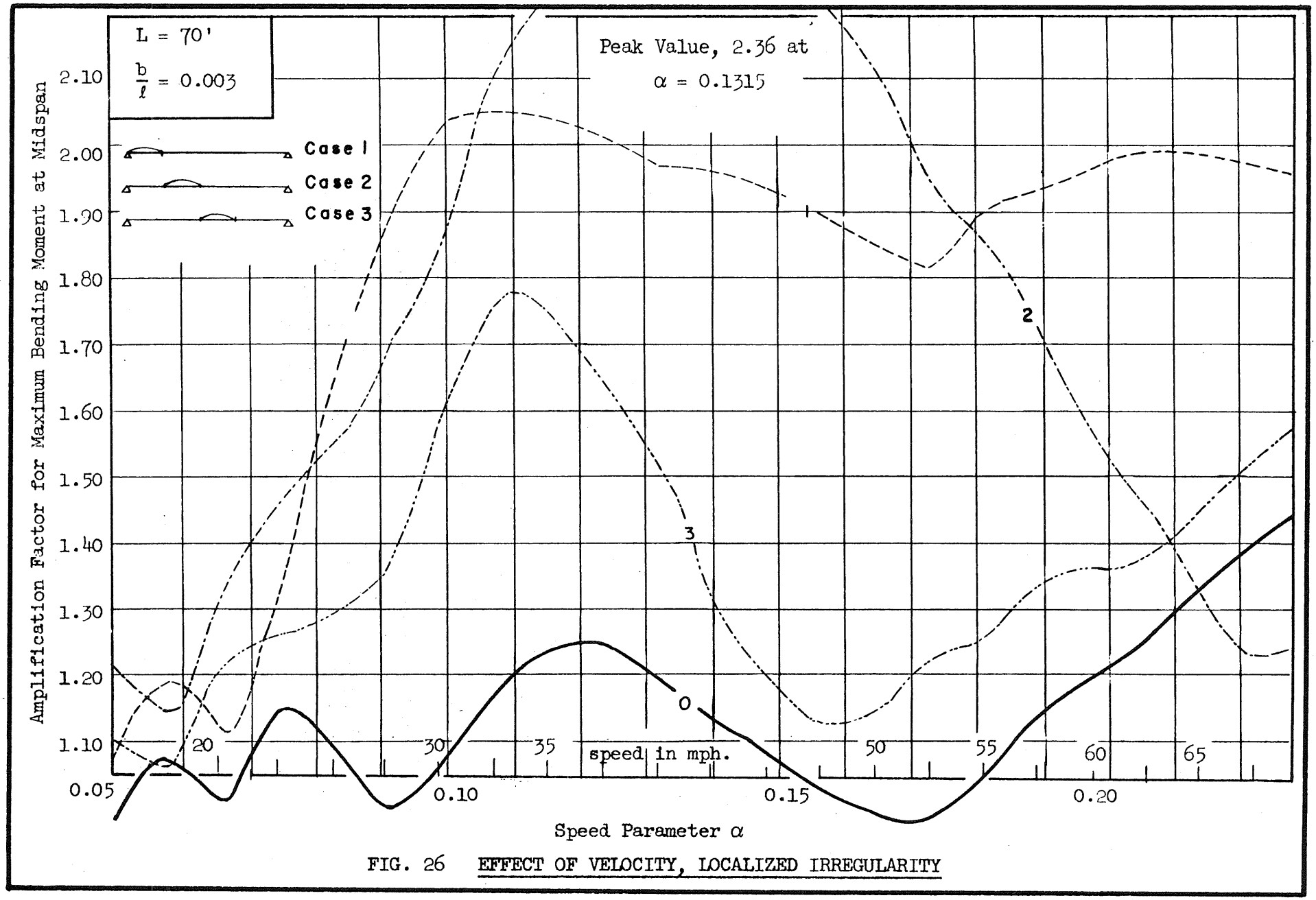

FIG. 26 EFFECT OF VELOCITY, LOCALIZED IRREGULARITY

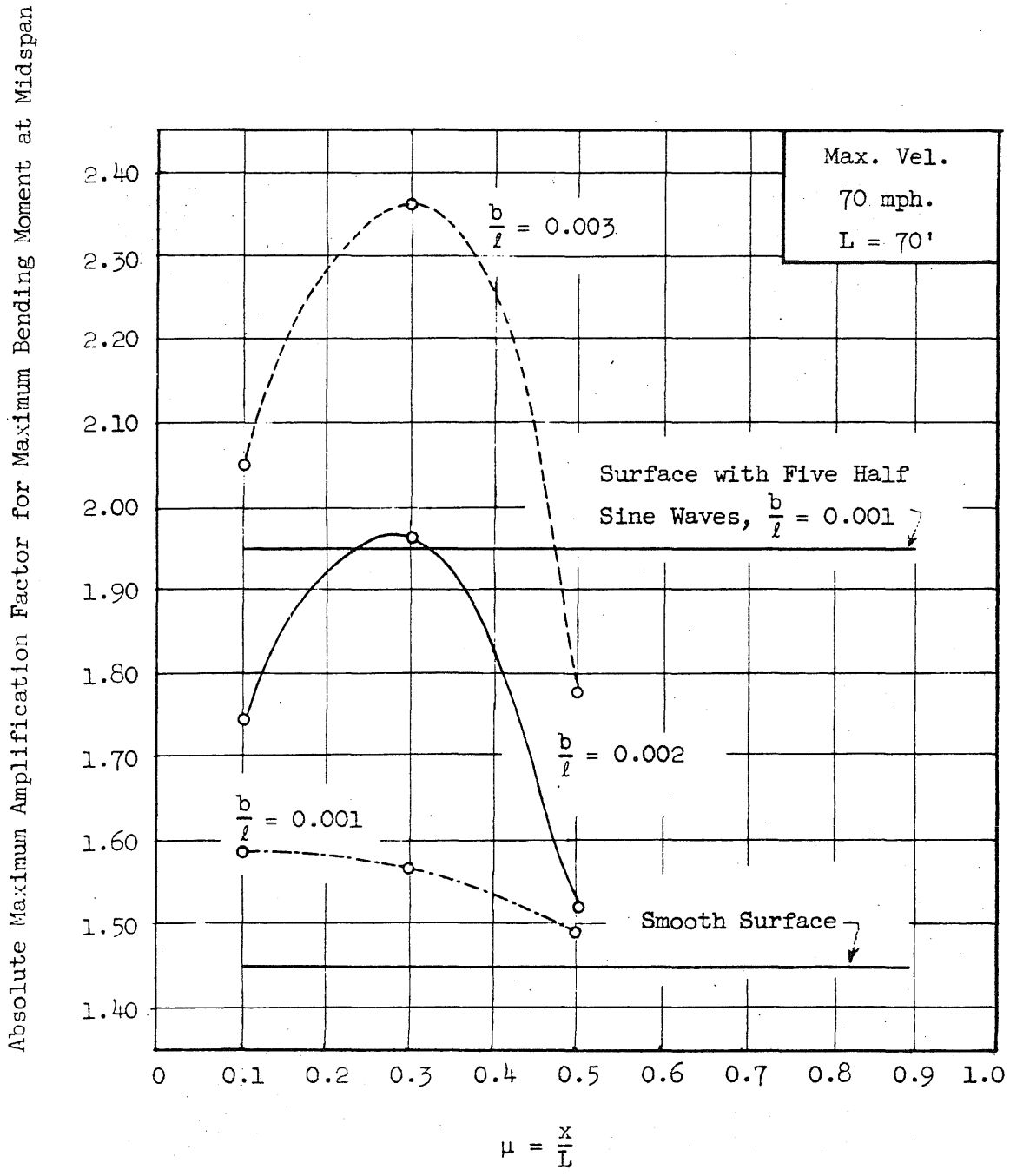

FIG. 27 ABSOLUTE MAXIMUM RESPONSE AT MIDSPAN,

LOCALIZED IRREGULARITY